AD_____

Award Number: W81XWH-F€ÌFËÐ F

TITLE: Ó^}:ã ãæ[|^Áæ ÁP[ç^|Á/@¦æ}ˆÁ[¦¦ÁP[¦{[}^ËÜ^¬æ&¦ˆÁT^æœ æœãÁÚ¦•æœ^ÁÔæ}&^¦

PRINCIPAL INVESTIGATOR: Qˆ ÁÔ@}*

CONTRACTING ORGANIZATION: V@ÁÔ@å¦^}ÔÁP[•]ãæ ÁÔ[¦][¦æã}
Ó[•q}Ë ÁT Œ/ÆGFFÍ Á

REPORT DATE: T æˆ ÁG€FF

TYPE OF REPORT: Annual Ù˘{{æ¦ˆ

PREPARED FOR: U.S. Army Medical Research and Materiel Command
Fort Detrick, Maryland 21702-5012

DISTRIBUTION STATEMENT: Approved for public release; distribution unlimited

The views, opinions and/or findings contained in this report are those of the author(s) and should not be construed as an official Department of the Army position, policy or decision unless so designated by other documentation.

REPORT DOCUMENTATION PAGE

Form Approved
OMB No. 0704-0188

1. REPORT DATE *(DD-MM-YYYY)*	2. REPORT TYPE	3. DATES COVERED *(From - To)*
01-05-2011	Annual Summary	15 APR 2010 - 14 APR 2011

4. TITLE AND SUBTITLE

Benzimidazole as Novel Therapy for Hormone-Refractory Metastatic Prostate Cancer

5a. CONTRACT NUMBER

5b. GRANT NUMBER
W81XWH-10-1-0241

5c. PROGRAM ELEMENT NUMBER

6. AUTHOR(S)

Ivy Chung

E-Mail: chungivy@hotmail.com

5d. PROJECT NUMBER

5e. TASK NUMBER

5f. WORK UNIT NUMBER

7. PERFORMING ORGANIZATION NAME(S) AND ADDRESS(ES)

The Children's Hospital Corporation
Boston, MA 02115

8. PERFORMING ORGANIZATION REPORT NUMBER

9. SPONSORING / MONITORING AGENCY NAME(S) AND ADDRESS(ES)
U.S. Army Medical Research and Materiel Command
Fort Detrick, Maryland 21702-5012

10. SPONSOR/MONITOR'S ACRONYM(S)

11. SPONSOR/MONITOR'S REPORT NUMBER(S)

12. DISTRIBUTION / AVAILABILITY STATEMENT
Approved for Public Release; Distribution Unlimited

13. SUPPLEMENTARY NOTES

14. ABSTRACT

The focus of this project is to evaluate the anti-tumor effects of benzimidazoles as a potential anti-metastatic prostate cancer therapy. We identified benzimidazoles, a class of anti-parasitic drug, in a drug screening process for preferential anti-tumor activity on metastatic prostate cancer cells. We demonstrated that benzimidazoles have potent anti-tumor activities, mediated through cell cycle arrest and induction of apoptosis. Our data indicates that benzimidazole treatment prolong the survival length of mice bearing prostate cancer metastases, inhibit the growth of prostate cancer cells growing in the bone microenvironment and more profoundly, remain active against paclitaxel-resistant prostate cancer tumors. This study further supports the use of benzimidazoles as potent anticancer therapy for men with metastatic prostate cancer.

15. SUBJECT TERMS
Benzimidazoles, anti-metastatic therapy, metastatic prostate cancer, apoptosis

16. SECURITY CLASSIFICATION OF:			17. LIMITATION OF ABSTRACT	18. NUMBER OF PAGES	19a. NAME OF RESPONSIBLE PERSON USAMRMC
a. REPORT U	b. ABSTRACT U	c. THIS PAGE U	UU	61	19b. TELEPHONE NUMBER *(include area code)*

Standard Form 298 (Rev. 8-98)
Prescribed by ANSI Std. Z39.18

Table of Contents

INTRODUCTION

The focus of this project is to evaluate the anti-tumor effects of benzimidazoles as a potential anti-metastatic prostate cancer therapy. We identified benzimidazoles, a class of anti-parasitic drug, in a drug screening process for preferential anti-tumor activity on metastatic prostate cancer cells. We have data indicate that benzimidazoles have potent anti-tumor activities, mediated through cell cycle arrest and induction of apoptosis. We have shown that treatment of benzimidazoles prolong the survival length of mice bearing prostate cancer metastases. This proposal will evaluate the effects of benzimidazoles in several *in vivo* mouse models of metastatic prostate cancer and delineate the mechanism(s) of action of benzimidazoles as novel anti-metastatic prostate cancer therapy.

Task 1: To determine the therapeutic efficacy of benzimidazoles in *in vivo* models of hormone refractory, metastatic prostate cancer

> 1a. Experimental human prostate cancer lymph node and bone metastases models

> 1b. Paclitaxel-resistant human prostate cancer cells model

> 1c. Anti-angiogenic and anti-lymphangiogenic activity in tumor vasculature of lymph node and bone metastases

Task 2: To dissect the role of ER stress in benzimidazoles-mediated apoptosis

> 2a. Ultrastructural and biochemical properties of benzimidazoles-induced ER stress

> 2b. Role of HERPUD1, ATF-3 and DDIT3 in benzimidazoles-induced apoptosis

BODY

1. **To determine the therapeutic efficacy of benzimidazoles in *in vivo* models of hormone refractory, metastatic prostate cancer:**

   1a) experimental human prostate cancer lymph node and bone metastases models
   Using the metastatic prostate cancer PC-3MLN4 cells that expressed luciferase, we investigated the anti-tumor effects of benzimidazoles in a model of experimental bone metastasis. Cells were inoculated directly into a single tibia of immunocompromised mice via intraosseous injection. When bone lesions were confirmed to be growing via bioluminescent imaging, mice were randomized and treated with vehicle or with 100 mg/kg albendazole for two weeks. As shown in **Appendix 1**, mice treated with albendazole showed reduced tumor growth compared to those treated with vehicle. There was a significant difference in average luciferase signal between the two groups over the course of treatment ($P < 0.05$) (**Appendix 2**). At the end

of study, the anatomical and radiographical characteristics of the bone lesions were evaluated with X-ray and micro-computerized tomography (CT) imaging. Mice treated with vehicle showed extensive osteolysis due to the osteoclastic bone resorption activity of PC-3MLN4 cells. In contrast, bone integrity was maintained in albendazole-treated mice (**Appendix 3 and 4**). These results demonstrated that the anti-tumor effects of benzimidazoles extend to tumors growing in intraosseuous spaces.

1b) paclitaxel-resistant human prostate cancer cells model

To evaluate whether benzimidazoles are effective against taxane-resistant cells, we treated two paclitaxel-resistant prostate cancer cells, PC-3TxR and DU-145TxR, with benzimidazoles. These cells, developed from PC-3 and DU-145 cells, respectively, were treated continuously *in vitro* with paclitaxel until significant resistance was developed [**1**]. These cells responded to the cytotoxic effects of benzimidazoles in a dose dependent manner, but were refractory to paclitaxel treatment (**Appendix 5**). In fact, benzimidazoles exhibited higher potency (lower ED50) in the paclitaxel-resistant cells than in the parental cells (**Appendix 6**). A significant cytotoxic effect was also observed with benzimidazoles in MES-SA/Dx5 human uterine sarcoma cells which are resistant to both microtubule stabilizer and disrupter agents (**Appendix 6**) [**2, 3**]. The observed cytotoxic activity correlated with the percent apoptosis induced in these cells (**Appendix 7**).

The anti-tumor activity of the benzimidazoles on paclitaxel-resistant cells was confirmed *in vivo*. PC-3TxR cells were inoculated subcutaneously in the flanks of the nude mice. When the tumors reached approximately 100 mm^3 in size, the mice were treated with vehicle, paclitaxel (10 mg/kg), fenbendazole (100 mg/kg) or albendazole (100 mg/kg) three times per week for 3 weeks. The benzimidazoles were prepared in DNTC and diluted with saline prior to injection. Compared to the vehicle treated group, the growth of PC-3TxR tumors in the paclitaxel group was significantly greater, indicating these cells require paclitaxel for optimal growth (**Appendix 8**). In contrast, tumors treated with either fenbendazole or albendazole were growth inhibited and remained at approximately 100-150 mm^3 in size throughout the study. These data strongly suggest benzimidazoles are effective against paclitaxel-resistant prostate cancer cells *in vitro* and *in vivo*.

1c) anti-angiogenic and anti-lymphangiogenic activity in tumor vasculature of lymph node and bone metastases

Both paraffin and frozen samples bone metastases in the animal studies performed in Aim 1a were collected and processed accordingly for further staining procedures. We were able to stain these samples for cell proliferation index Ki-67 (a replacement for the proposed PCNA) and apoptotic marker caspase-3. Imunohistochemical analysis of these bone lesions further showed a reduction of Ki-67 labeling index (*P*<0.005) and an increase of apoptotic index, based on activated caspase-3 staining (*P*<0.005) in the albendazole-treated group (**Appendix 9**). These results strongly support our hypothesis that the *in vivo* anti-tumor

effects of benzimidazoles are mediated partly by inhibition of cell proliferation and induction of apoptosis.

The staining procedure for endothelial cell marker (CD31) and lymphangiogenic marker (LYVE1) were under optimization; therefore no samples have been successfully stained and analyzed with these markers.

2. **To dissect the role of ER stress in benzimidazoles-mediated apoptosis**

    2a. Ultrastructural and biochemical properties of benzimidazoles-induced ER stress

    2b. Role of HERPUD1, ATF-3 and DDIT3 in benzimidazoles-induced apoptosis

No report available due to early termination of the award.

KEY RESEARCH ACCOMPLISHMENT

- Benzimidazole treatment demonstrates significant anti-tumor activity in an experimental model of bone metastases, by reducing bone osteolysis as observed with radiographic imaging.
- Benzimidazoles showed potent anti-tumor activity on paclitaxel-resistant prostate cancer cells *in vitro* and *in vivo*, with higher potency in ED50 when compared to paclitaxel-sensitive cells and inhibition of subcutaneously growing tumor *in vivo*.
- The anti-tumor effects of benzimidazole are partly mediated by induction of apoptosis and inhibition of angiogenesis.

REPORTABLE OUTCOMES

- Poster presentation at 101th American Association of Cancer Research Annual Meeting at Washington DC in April 2010. Title: Benzimidazoles as novel therapeutic agent for metastatic prostate cancer
- Poster presentation at Judah Folkman's Research Day at Children's Hospital Boston, MA in March 2010. Title: Development of anti-parasitic drugs in targeting metastatic prostate cancer.
- Manuscript in preparation for submission to Journal of National Cancer Institute. Title: (see **Appendix 10**).

CONCLUSIONS:

Benzimidazoles were identified from a screen that selectively target highly metastatic prostate cancer cells but not toxic to normal cells. We determined that the preferential anti-tumor activity of these agents was mediated partly through cell cycle arrest and induction of apoptosis, both in vitro and in vivo. We further demonstrate that benzimidazole treatment prolongs the survival of mice bearing prostate cancer lung metastases and inhibit the growth of prostate cancer cells growing in the bone microenvironment. More strikingly, these anti-tumor effects remain active against prostate cancer cells that are resistant to paclitaxel, the standard chemotherapy for men with advanced prostate cancer, both in vitro as well as in vivo. Our study further supports the use of benzimidazoles as potential anti-cancer therapy for men with metastatic prostate cancer.

REFERENCES:

1. Takeda M, Mizokami A, Mamiya K, Li YQ, Zhang J, Keller ET, Namiki M. The establishment of two paclitaxel-resistant prostate cancer cell lines and the mechanisms of paclitaxel resistance with two cell lines. Prostate 2007; 67: 955-67.

2. Leoni LM, Hamel E, Genini D, Shih H, Carrera CJ, Cottam HB, Carson DA. Indanocine, a microtubule-binding indanone and a selective inducer of apoptosis in multidrug-resistant cancer cells. J Natl Cancer Inst 2000; 92: 217-24.

3. Scudder SA, Brown JM, Sikic BI. DNA cross-linking and cytotoxicity of the alkylating cyanomorpholino derivative of doxorubicin in multidrug-resistant cells. J Natl Cancer Inst 1988; 80: 1294-8.

APPENDIX 1:

Bone lesions of PC-3MLN4 cells were generated by intraosseous injection into the tibia of mice, before treatment with vehicle or 100 mg/kg albendazole (ABZ), given intraperitoneally, three times a week for two weeks. Representative photos of luciferase signal detected in each treatment group at the beginning and end of study.
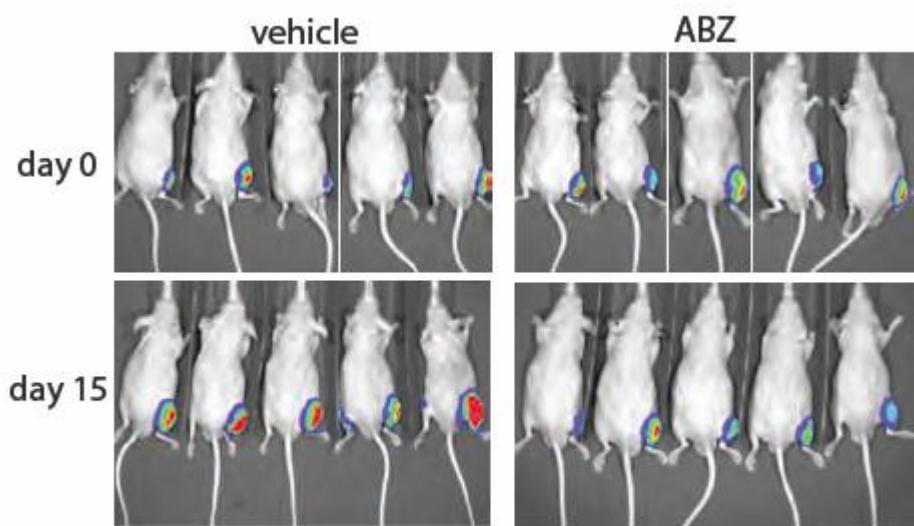
APPENDIX 2:

Bone lesions of PC-3MLN4 cells were generated by intraosseous injection into the tibia of mice, before treatment with vehicle or 100 mg/kg albendazole, three times a week for two weeks. Mean of luciferase signals detected in mice during the course of treatment, as a measurement of tumor burden. Data shown are mean ± 95% confidence interval, N=10 per group.
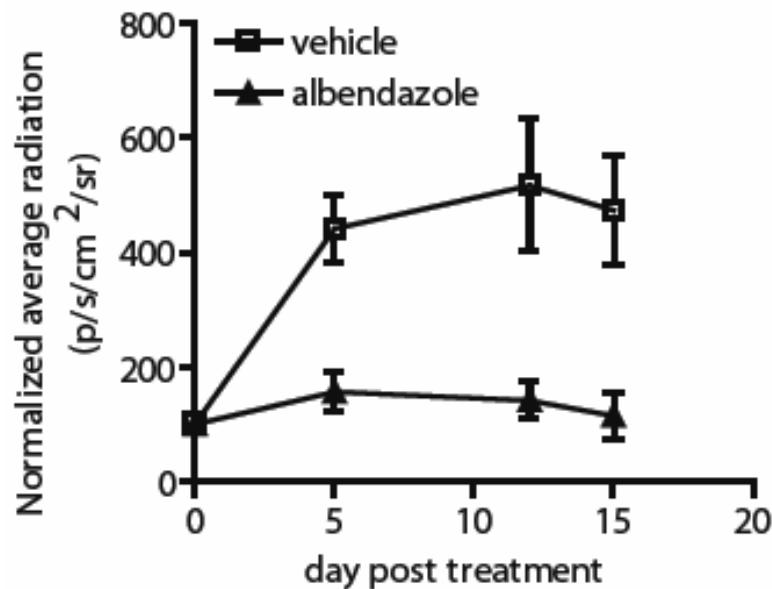
APPENDIX 3:

Bone lesions of PC-3MLN4 cells were generated by intraosseous injection into the tibia of mice, before treatment with vehicle or 100 mg/kg albendazole, three times a week for two weeks. Representative images from X-ray analysis show differences in anatomical and radiographical characteristics of the bone lesions.
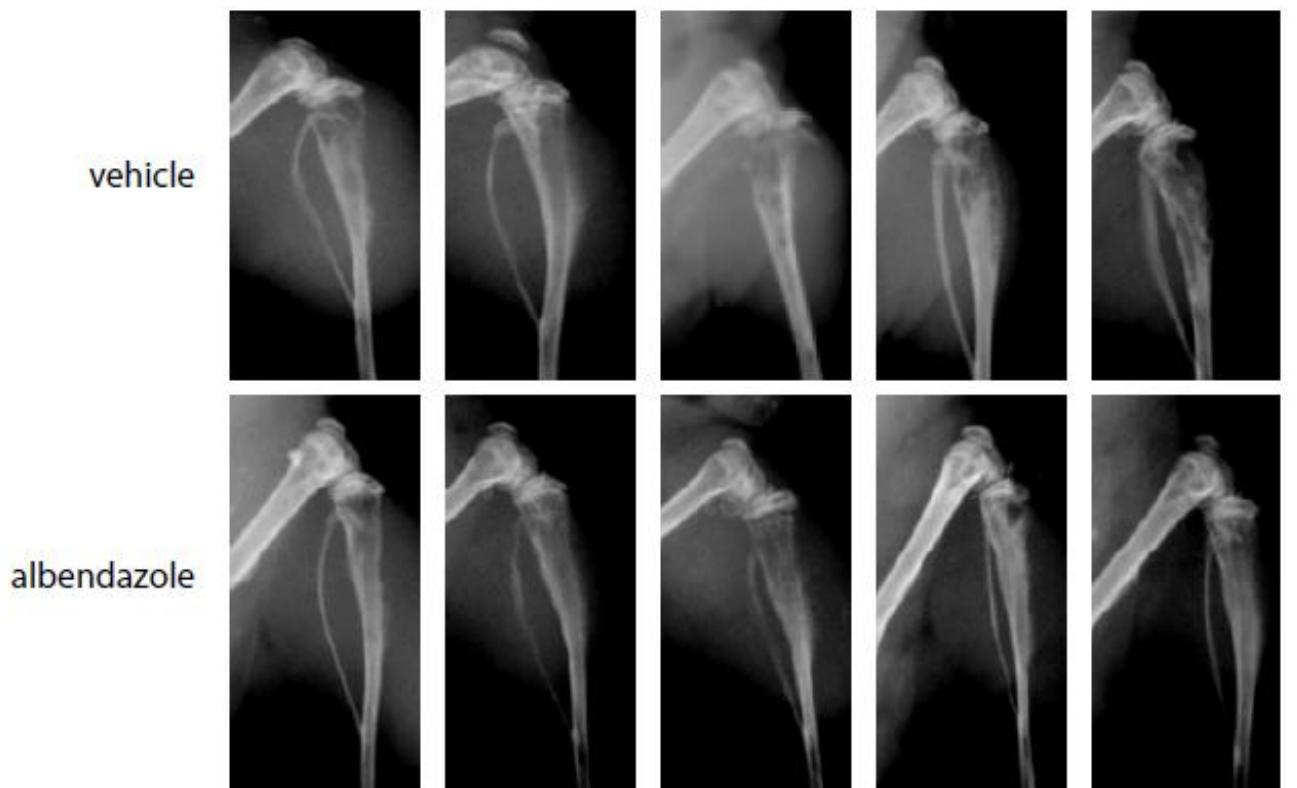
APPENDIX 4:

Bone lesions of PC-3MLN4 cells were generated by intraosseous injection into the tibia of mice, before treatment with vehicle or 100 mg/kg albendazole, three times a week for two weeks. Representative images from micro-CT analysis show differences in anatomical and radiographical characteristics of the bone lesions.
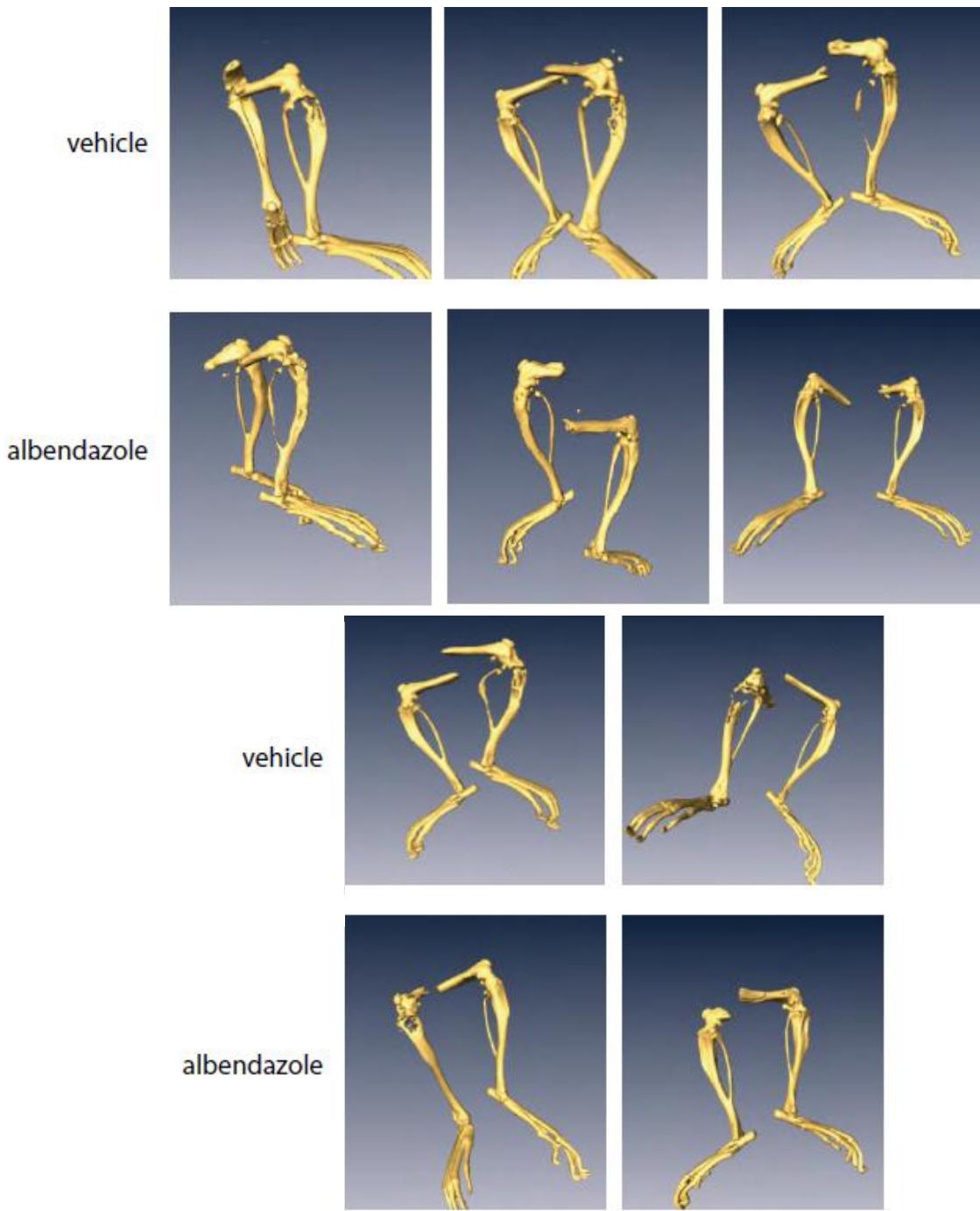
APPENDIX 5:

Cytotoxic effects of paclitaxel and fenbendazole (FBZ) in paclitaxel-resistant prostate cancer cells, PC-3TxR (A) and DU-145-TxR (B). Cytotoxicity for 72 hour treatment was measured using Cyquant cell proliferation assay. Data shown are mean ± 95% confidence interval, N=4 per group.
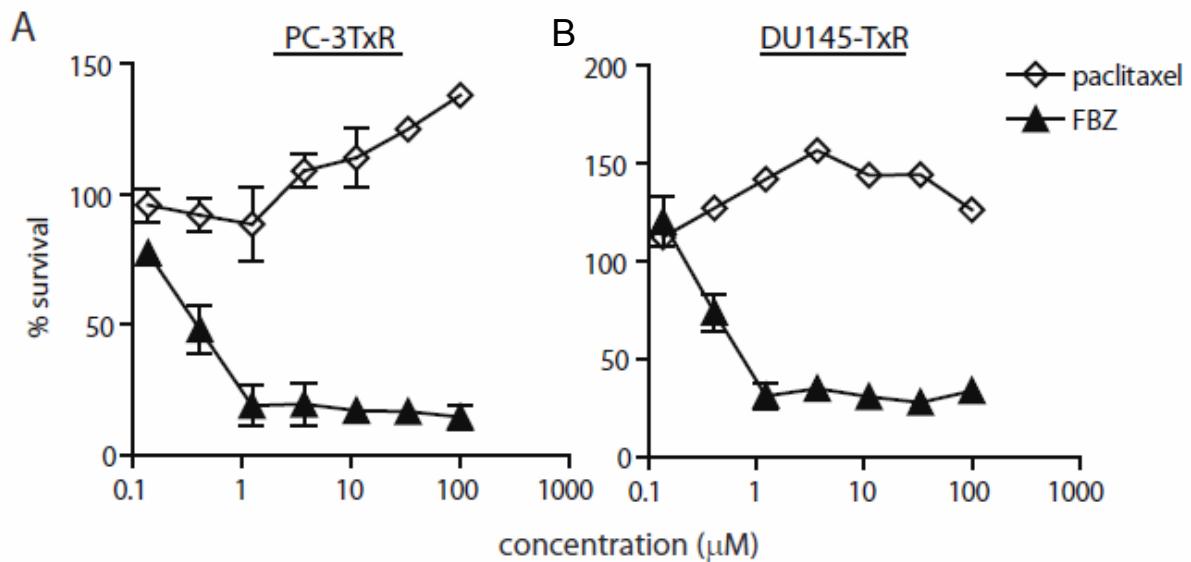
APPENDIX 6:

Cytotoxic effects of paclitaxel and benzimidazoles in paclitaxel-resistant prostate cancer cells, PC-3TxR (A) and DU-145-TxR (B). Cytotoxicity for 72 hour treatment was measured using Cyquant cell proliferation assay. Shown are comparison of ED50 of agents in paclitaxel-sensitive and –resistant prostate cancer cell lines.

Compound	ED50 (μM)					
	PC3	PC-3TxR	DU145	DU145-TxR	MESSA	MESSA DX5
Fenbendazole	1.57	0.32	10.7	4.21	3.04	1.13
Albendazole	4.86	0.80	2.41	1.08	1.48	0.48
Mebendazole	2.85	0.79	5.90	2.97	3.21	1.67
Carbendazim	NT	NT	NT	NT	NT	NT

APPENDIX 7:

Cytotoxic effects of paclitaxel and benzimidazoles in paclitaxel-resistant prostate cancer cells, PC-3TxR and DU-145-TxR in comparison with the sensitive counterparts, PC-3 and DU-145, respectively. Percent apoptosis induced by each agent in paclitaxel-sensitive and –resistant cell lines, as measured by annexin V staining. Data shown are mean ± 95% confidence interval, N=4 per group.

Compound	% apoptotic cells (72 hr)			
	PC3	PC-3TxR	DU145	DU145-TxR
Vehicle	8.1	10.1	9.6	9.0
Paclitaxel (100 nM)	16.4	8.9	37.3	11.5
Fenbendazole (1µM)	16.1	34.4	26	43.3
Albendazole (1µM)	13.2	25.8	27	55.8
Mebendazole (1µM)	11.9	21.5	16.4	36.7
Carbendazim (1µM)	6.12	7.09	5.78	6.34

APPENDIX 8:

PC-3TxR paclitaxel-resistant prostate cancer cells were inoculated subcutaneously into the flanks for nude mice, before treatment with either vehicle, paclitaxel 10 mg/kg or fenbendazole (FBZ) 100 mg/kg, three times a week for three weeks. (*Left*) Relative growth of subcutaneous PC-3TxR tumors after treatment with DNTC alone, paclitaxel or FBZ. (*Right*) Average of tumor size from each treatment group at the end of study. Data shown are mean ± 95% confidence interval, N=10 per group.
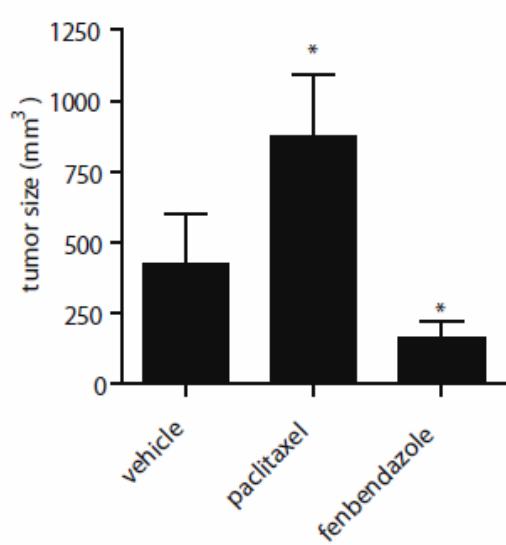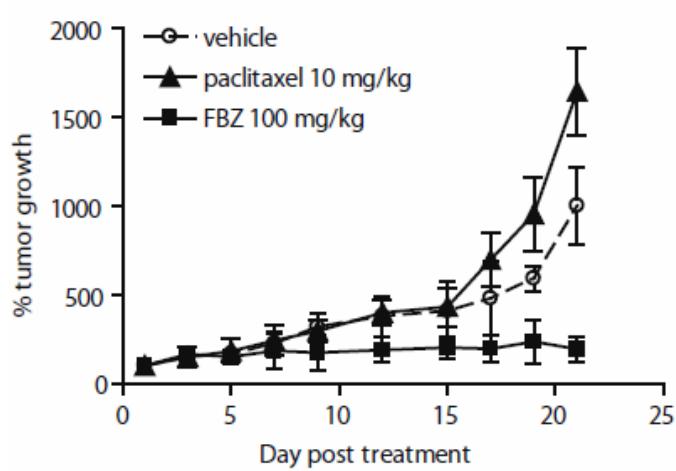
APPENDIX 9:

Effects of albendazole on metastatic prostate cancer bone lesions in the mouse. PC-3LN4 cells were inoculated intraosseously into the tibia of the mouse. After two weeks when bone lesions were confirmed growing, mice were treated with either vehicle or 100 mg/kg albendazole for three weeks. Upon completion of treatment, bone lesions were harvested and stained for cell proliferation marker (Ki67) and apoptotic marker (caspase-3). (A) Shown are representative H&E, Ki67 and caspase-3 stained specimen from each group. (B-C) Staining intensity on each specimen were quantified using Aperio image digital software. Data shown are mean ± 95% confidence interval, N=10 per group. *, $P<0.01$ by ANOVA test.
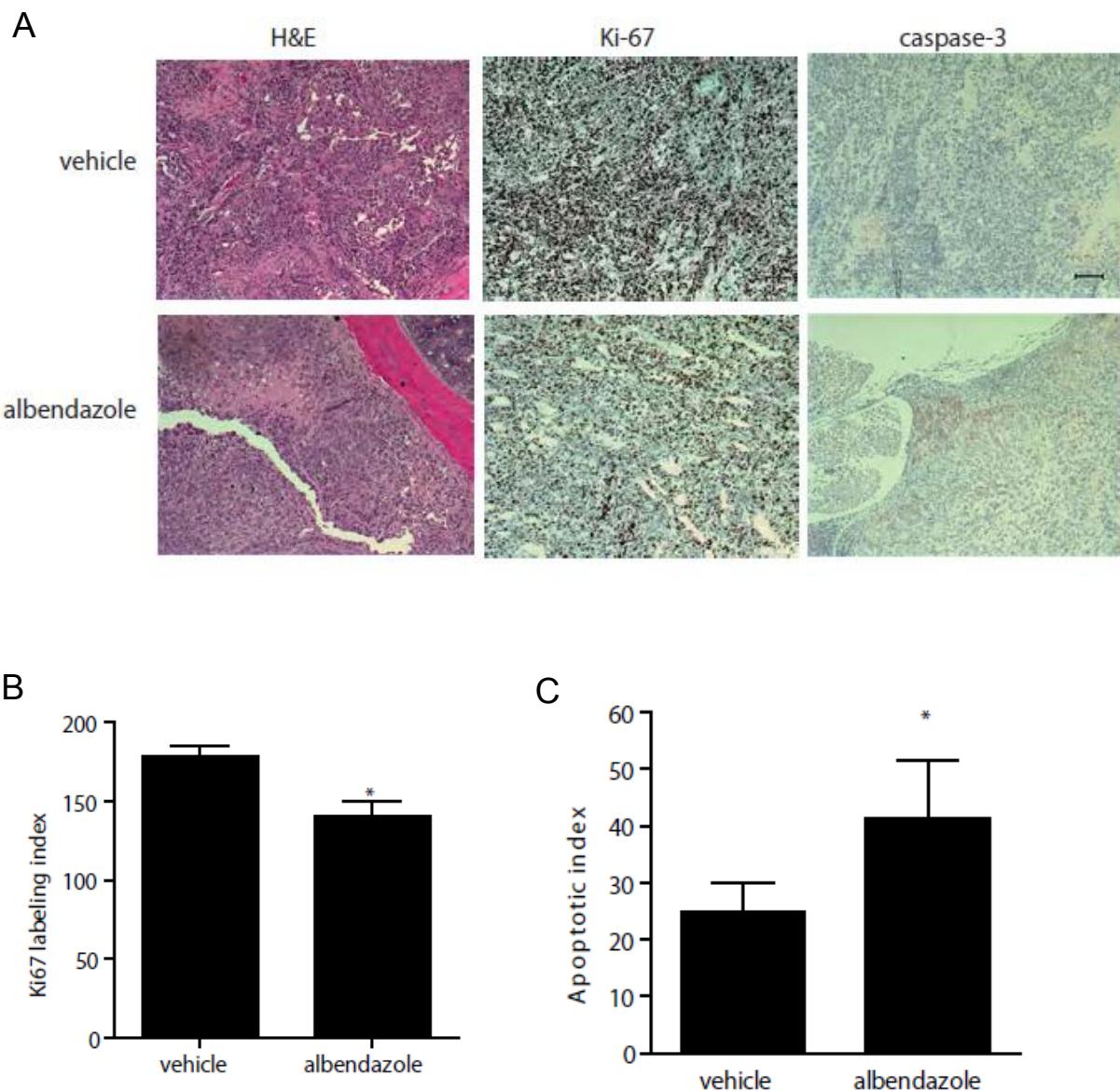
APPENDIX 10:

Manuscript in preparation for submission to Journal of National Cancer Institute.

Title: Identification of selective therapeutic agents for metastatic prostate cancer by phenotype-based screening

Authors and affiliation:

Ivy Chung[1], Courtney Barrows[1,5], Jacqueline Banyard[1], Arianne Wilson[1], Nathan Rummel[2], Atsushi Mizokami[3], Sudipta Basu[4], Poulomi Sengupta[4], Badaruddin Shaikh[2], Shiladitya Sengupta[4], Diane R. Bielenberg[1] and Bruce R. Zetter[1*]

[1]Vascular Biology Program, Children's Hospital Boston and Department of Surgery, Harvard Medical School, [2]Food and Drug Administration's Center for Veterinary Medicine, [3]Department of Integrative Cancer Therapy and Urology, Kanazawa University Graduate School of Medical Sciences, Kanazawa, Ishikawa, Japan, [4]Laboratory for Nanomedicine, Department of Medicine, Brigham and Women's Hospital.

[5]Present address: New York Medical College, Valhalla, NY 10595

*Corresponding author: Bruce R. Zetter, Vascular Biology Program, Children's Hospital Boston, Karp Family Research Laboratories 11.125, 300 Longwood Avenue, Boston, MA 02115, USA. Tel: (617) 919-2320, Email: bruce.zetter@childrens.harvard.edu

ABSTRACT

Background: As with many solid tumors, the prognosis for prostate cancer patients worsens when tumors metastasize to distant organs, such as the bone. Current chemotherapy is relatively limited for metastatic prostate cancer.

Methods: We utilized a screening method consisting of multiple panels of highly metastatic and less metastatic prostate cancer cells to identify compounds that selectively target metastatic prostate cancer cells but not on less metastatic and normal prostate epithelial cells. Selected drugs from a library of 1120 FDA-approved drugs were then tested for their ability to improve the survival of mice in a highly aggressive Dunning rat prostate carcinoma lung metastasis model, and for anti-tumor activity on paclitaxel-resistant and experimental bone lesion of prostate tumors. To improve the bioavailability of agents for systemic administration, we utilized a modified micelle preparation as well as nanoparticle (PLGA-PEG)-based formulation.

Results: We identified fenbendazole, fluspirilene, clofazimine, niclosamide and suloctidil, which showed selective cytotoxicity on metastatic prostate cancer cells in vitro and in vivo. Such selectivity could explained by differential induction of apoptosis. Upon improvement in bioavailability, fenbendazole and albendazole significantly extended the survival of metastases-bearing mice, and the extension of lifespan by albendazole was equivalent or greater than that provided by paclitaxel. These drugs were active in taxane-resistant tumors and in the bone microenvironment, two clinical conditions of men with advanced prostate cancer.

Conclusion: Metastatic tumor cells differ in their responses to certain drug classes. Albendazole shows promise as a potential adjunct to standard therapy in patients with metastatic prostate cancer.

INTRODUCTION

In the United States, prostate cancer is second only to lung cancer as a cause of cancer-related deaths in men (1). Mortality from prostate cancer is largely restricted to patients with disseminated metastases in bone or in other distal sites. Despite a generally high five-year survival rate of 80% for localized disease (2), approximately 25% of prostate cancer patients develop metastatic disease following surgery or radiation therapy (3, 4). Although androgen ablation is often effective as an initial treatment for recurrent prostate cancer, the disease almost inevitably progresses to a hormone-refractory state. Men with hormone-refractory disease have a poor prognosis, with median survival times of 9 to 12 months (5). In addition, the morbidity associated with this disease is significant, including spinal cord compression, fractures, pain, and ultimately, death. The management of hormone refractory metastatic prostate cancer has been limited to palliation of symptoms due to a lack of effective treatments. Recently, taxane-based chemotherapy was shown to improve survival in men with metastatic disease (6, 7). Although most patients initially respond to paclitaxel, the majority of these cancers eventually develop resistance, resulting in a more aggressive, chemotherapy-resistant disease (8). There is an urgent need to find alternative treatments designed to prolong survival of patients with metastatic prostate cancer.

It is widely observed that metastatic lesions in many cancers respond poorly to existing therapies, including chemo- and radiation therapy. The reason for this is not clear. It may be due simply to the extent of the metastatic burden. Alternatively, metastatic tumor cells may possess specific properties that render them refractory to treatments that are effective against less aggressive tumors. Studies have demonstrated that these metastatic tumor cells may acquire stem cell properties including expression of certain cell-surface markers (9, 10), and therefore

3

exhibit increased resistance to chemotherapeutic agents and ionizing radiation (11). Likewise, during the evolution of metastatic progression, these cells may also acquire vulnerabilities or susceptibility to certain agents. We hypothesized that such vulnerabilities could be targeted in developing effective agents for treatment of metastatic prostate cancer.

To test this hypothesis, we employed multiple panels of highly metastatic and poorly metastatic prostate cancer cells to determine whether they were differentially responsive to a library of 1120 drugs, most of which are Food and Drug Administration-approved drugs. Intriguingly, we found that several drugs demonstrate greater cytotoxicity against tumor cells with greater metastatic potential in both in vitro and in vivo assays. Because these drugs are already used in humans for different purposes, such newly discovered agents can quickly enter human clinical efficacy studies using the existing drug administration regimen, or be improved based on the known pharmacokinetic and pharmacodynamic profiles. Our work demonstrates that it is possible to conduct a screen for drugs that can effectively treat metastatic tumors and further suggests that these newly identified agents may be examples of "recycled drug" approach in drug development.

MATERIALS AND METHODS

Chemical and Reagents

Drugs in the drug library were solubilized in DMSO. The following chemicals were purchased from Sigma Aldrich: fenbendazole (F5396), albendazole (A4673), fluspirilene (F100), clofazimine (C8895), niclosamide (N3510), suloctidil (S9384), tween-80 (P4780), N-methyl-2-pyrrolidone (NMP) (328634) and cremophor EL (Cr-EL) (C5135). Paclitaxel were purchased from Cytoskeleton (for in vitro) or Bristol-Meyer (for in vivo). Gaussia luciferase system was

purchased from Targeting Systems (LP-07). Caspase inhibitor Z-VAD-FMK and Matrigel were purchased from MP Biomedical (03FK10901) and BD Biosciences (354323), respectively.

Cell culture

PC-3M and PC-3MLN4 human prostate cancer cells were provided by I. Fidler (12), AT6.1 rat prostate carcinoma cells were provided by J. Isaacs (13) and rat prostate epithelial nBE cells (14) were provided by M. Freeman. MESSA, MESSA-Dx5 and DU-145 were obtained from the American Type Culture Collection. PC-3TxR and DU-145TxR cells and the sensitive counterparts were provided by A. Mizokami (15). All PC-3 and DU-145 derivative cell lines were maintained in RPMI 1640 and DMEM, respectively, supplemented with 10% fetal bovine serum and 1% penicillin/streptomycin.

DU-145LN4 human prostate cancer cell model

DU-145 human prostate cancer cells were injected orthotopically in nude mice, and paraaortic lymph node metastases were established in culture with the first line called DU-145LN1. This process was repeated four cycles to establish DU-145LN4. When compared, DU-145LN4 cells demonstrate greater incidence of lymph node metastases (75-100%) than DU-145 cells (0%).

Synthesis of DNTC and pegylated nanoparticle formulation

Compounds were prepared either in 100% DMSO or in a mixture of DMSO, NMP, tween-80 and cremophor EL (DNTC) in a 1:3:2:2 ratios. The resultant mixture was stable and was stored in room temperature. Nanoparticles were formulated using an emulsion-solvent evaporation technique and PLGA-PEG conjugate was synthesized as published in (16). 40 mg PLGA (MW = 4.2 kD) and 10 mg of PLGA-PEG were dissolved completely in 2.5 mL acetone

and mixed with 5 mg of albendazole.   The entire solution was emulsified into 25 mL of 2%
aqueous solution of PVA (80% hydrolyzed, Mw~ 9000-10,000) by slow injection with constant
homogenization using a tissue homogenizer. This mini emulsion was added to a 100 mL 0.2%
aqueous solution of PVA (80% hydrolyzed, Mw ~ 9000-10,000) with rapid mixing for 4h at
room temperature to evaporate any residual acetone. NP size fraction was recovered by
ultracentrifugation at 3,000 x g for 5 minutes and 90,000 x g for 2h. The size distribution of
nanoparticles was studied by dynamic light scattering (DLS), which was performed at 26˚C on a
Malvern Zetasizer DLS-system equipped with a He-Ne laser. The albendazole loading in the NPs
was determined by UV-VIS spectroscopy at the wavelength $\lambda = 298$ nm.

Physicochemical release kinetics characterization of ABZ Nanoparticles

Albendazole NPs were suspended in 500 µL of AT6.1 cell lysate and sealed in a dialysis
bag (MWCO ~ 1000 Da). The dialysis bag was incubated in 1 mL of PBS buffer at room
temperature with gentle shaking. 10 µL of aliquot was extracted from the incubation medium at
predetermined time intervals, dissolved in 90 µL DMF and released albendazole was quantified
by UV-VIS spectroscopy at characteristic wavelength of albendazole, $\lambda = 298$ nm. After
withdrawing each aliquot the incubation medium was replenished by 10 µL of fresh PBS.

Cytotoxicity assay and ED50 determination

Cell survival assay using Cyquant reagent (Invitrogen, C7026) was performed as
described (17). Briefly, 1-4 x 10^5 cells were seeded in 96 well plate overnight, before treatment
with either vehicle or drug for 48-72 hours. Cells were harvested, washed and freezed at -80 °C
overnight. After thawing to room temperature, Cyquant reagent was added and fluorescence
intensity was read with a spectrometer at 485 nm. Percent survival was calculated by dividing
the reading from drug-treated cells by the reading from vehicle-treated cells. Median-dose effect

analysis and ED50 calculation (50% reduction in cell survival) was performed using CompuSyn software (ComboSyn, Inc.), as described previously (18).

Annexin V/7-amino-actinomycin D staining

Annexin V/7-amino-actinomycin D labeling was performed according to the manufacturer's instructions (BD Pharmingen, 559763) and samples were analyzed by flow cytometry. Briefly, cells were treated for 72 hours with either vehicle or compounds, with or without 20 µM z-VAD-FMK caspase inhibitors. Cells were trypsinized, washed and resuspended in assay binding buffer, labeled with annexin V and 7-amino-actinomycin before analysis by flow cytometry (BD FACScan). Apoptotic cell population was determined by the mean of positive staining of annexin V from three replicates. Data shown were representative of three independent experiments.

Measurement of benzimidazole metabolites

Mice were given a bolus injection of 50 or 150 mg/kg drug prepared in DMSO or DNTC formulation before collection of plasma samples eight hours post injection. Benzimidazoles and their active metabolites (both sulfones and sulfoxides) in the plasma were extracted by liquid-liquid partition using potassium carbonate, DMSO, sodium metabisulfite and ethyl acetate, dried and analyzed by high performance liquid chromatography (HPLC) on a 150 x 4.6 mm Phenomenex Luna C18 5-µ column. Fenbendazole and its metabolites were detected using UV light (290 nm), while albendazole and its metabolites were detected using fluorescence (excitation at 290 nm; emission at 330 nm).

In vivo drug treatment studies

Inbred male nu/nu mice age 6-8 weeks were obtained from Massachusetts General

Hospital (Boston, MA). The mice were virus antibody free, age and weight matched for experimental use and fed with a balanced rodent diet ad libitum. 1×10^4 log-phase AT6.1 cells were injected via tail vein in 0.1 mL Hanks solution. On day 5 post inoculation, treatment was begun and continued three times per week via intraperitoneal injection in 0.5 mL volume. Drugs were prepared with either DMSO alone, DNTC vehicle or PLGA-PEG vehicle and diluted in saline prior to injection. During the course of treatment, the mice were monitored for toxicity as evidenced by body weight loss. Treatment was continued until the animals showed signs of morbidity defined by significant loss of body weight, difficulty in breathing and hunched posture.

PC-3MLN4 (2 million) cells were injected directly into the tibia of the mice in 0.1 mL Hanks solution, using method as described by Berlin O et al (19). Bone lesions were monitored weekly by bioluminescent imaging (Xenogen IVIS™, Xenogen, CA). Two weeks post injection, mice with comparable tumor lesions were randomly divided into two groups for treatment of either vehicle or 100 mg/kg albendazole, given intraperitoneally three times per week for two weeks. Bioluminescent imaging was performed on these mice once a week and bioluminescence signals were used as a measure of the tumor size. At the end of the study, radiographical and anatomical changes of the bone lesions were obtained using X-ray (Faxitron X-Ray, IL) and micro-computed tomography (Siemens CAT II scanner, Siemens, NY).

PC-3TxR cells were maintained in culture as described above before harvested for injection. 2 million cells were injected subcutaneously into the flank of mice in 0.5 mL Hanks solution containing Matrigel (1:1). When the tumors reached approximately 100 mm^3 in size, treatment began and continued three times a week as described above. Tumor volume was measured using a caliper and calculated with the formula: Volume = Length x Width^2 /2.

Relative tumor growth was determined by normalizing the tumor size at each time point with the initial size prior to the start of treatment. Animals were euthanized with CO_2 and tissues were collected for further analysis. The animals and experiments used in these studies were approved by the institutional animal care committee according to Children's Hospital Boston ARCH guidelines.

Measurement of blood Gaussia luciferase assay

Blood Gaussia luciferase assay was performed as described in (20). Briefly, 10-20 µL peripheral blood was collected from the animals once a week via retro-orbital vein. Secreted GAR luciferase activity was measured using a luminometer by adding 100 µL of 100 µM coelentrazine (Prolume, Nanolight, #303) to 5 µL blood with addition of 2 µL of 20 mM EDTA. The relative luciferase reading from the blood collected represents the tumor burden in each animal.

Immunohistochemical staining and scoring

Tissues were collected and fixed in formalin before processing for paraffin embedding. Tissue sections were then processed for Ki-67 and caspase-3 antibody staining, performed by Dana Farber Cancer Institute/Harvard Cancer Center Research Pathology Core. The staining were performed using Ki-67 antibody (DAKO, M7248) and caspase-3 antibody (Cell Signaling, 9664S), followed by detection methods using streptavidin HRP and rabbit ENVISION (DAKO), respectively. The immunostained slides were scanned using an Aperio CS Scanner (Vista, CA) at 20x magnification. Using Imagescope v10, at least 50 digital images of areas containing the tumor cell only were randomly selected from 8 tissues to represent each treatment group. Ki-67 and caspase-3 staining intensity were scored using validated IHC nuclear image and color deconvulated algorithms, respectively. Intensity was scored as 0 for absence of staining, 1+ for

weak, 2+ for moderate, and 3+ for strong staining. Based on the percentage of these intensities, a score is determined with the formula: Score = (1.0 x %weak) + (2.0 x %moderate) + (3.0 x % strong). Both necrotic and peripheral tissue areas were excluded from the analysis.

Statistical analysis

All values are expressed as means ± 95% confidential interval (CI). For comparisons between two groups, statistical significance was assessed with a two-tailed unpaired Student's t test. The computations and graphs were performed and constructed with the GraphPad Prism 4.0 scientific graphing, curve fitting and statistics program (GraphPad Software, CA).

RESULTS

Screening for selective cytotoxic agents against metastatic prostate cancer

We evaluated the cytotoxic effects of 1120 compounds from a commercialized chemical drug library in several phases of in vitro screening (Fig. 1A). In the first phase, drugs were selected based on preferential toxicity against highly metastatic human prostate cancer cells PC-3MLN4 relative to the less aggressive counterpart, PC-3M (13). Cells were treated with a fixed concentration (10 µM) for 48 hours and analyzed for remaining viable cells. A drug was considered a "hit" if it resulted in a) a significantly greater growth inhibition in PC-3MLN4 than in PC-3M cells; or b) at least 80% growth inhibition in both of the cell lines. 44 of the drugs were identified as "hits" and were taken into the second line of screening, in which these drugs were tested in a range of concentrations for 48 hours in PC-3M/PC-3MLN4, as well as in a second pair, DU-145/DU-145LN4 (Screen II). DU-145LN4 is a metastatic variant established from lymph node metastases after injection of DU-145 cells into the mouse prostate. "Hits" from this screen were defined when a drug showed preferential cytotoxicity in both of the

metastatic variants with at least 50% growth inhibition and a significant difference (P<0.05) when compared to the parental counterpart, for at least two of the concentrations tested. 23 drug candidates (2% of the total library) were considered a "hit" in this screen.

To prepare for in vivo testing, the positive candidates were tested next in a highly aggressive Dunning rat prostatic adenocarcinoma AT6.1 model (Screen III). AT6.1 cells develop lymph node and lung metastases when inoculated subcutaneously in rats or in immunocompromised mice (21, 22). In this screen, cells were treated with drugs over a range of concentrations for 48 hours; drugs were designated when they caused more than 40% growth inhibition in at least two concentrations tested.

To further increase the stringency of our screening process, the 10 drugs that passed through Screen III were tested for minimal cytotoxic effects to normal host cells (more than 90% survival) using non-tumorigenic rat prostate epithelial nBE cells (Screen IV). From this screening sequence, we finally identified five candidate drugs: clofazimine, fenbendazole, fluspirilene, niclosamide and suloctidil, that selectively exert cytotoxic effects on all metastatic prostate cancer cell lines tested but not on normal rat epithelial cells. For example, treatment of 1 µM fenbendazole resulted in 69% (95% CI=67.04 to 70.96%) and 65% (95% CI=64.02 to 65.98%) growth inhibition in the highly metastatic PC-3MLN4 and DU-145LN4 cells, respectively, when compared to 46% (95% CI=42.08 to 49.92%) in poorly metastatic PC-3M cells and 49% (95% CI=47.04 to 50.96%) in DU-145 cells (Fig. 1B). Fenbendazole at 1 µM concentration also exhibited increased cytotoxicity in the highly aggressive AT6.1 cells (53.2% growth inhibition, 95% CI=51.7 to 54.6%) but not in the normal prostate epithelial nBE cells (0% growth inhibition, 95% CI=-2 to 2%) (Fig. 1B).

Fenbendazole and niclosamide, both anti-helminthic agents, are widely used in veterinary medicine (23) and in treating tapeworm infection in human (24), respectively. Clofazimine is currently used for treatment of leprosy whereas flusprilene is used in the treatment of schizophrenia (25, 26). Suloctidil, a vasodilator, was formerly used in the management of peripheral and cerebral vascular disorders (27). Identification of these agents in our multi-stage in vitro screen prompted us to investigate their potential anti-tumor activity in vivo.

In vivo screening of lead drugs in a survival model of lung metastasis

Many anti-tumor drugs are tested only for their ability to prevent primary tumor growth or to prevent the dissemination of metastatic cells. Therefore, the drug is usually administered shortly after the primary tumor is established. To effectively treat metastatic cancer, a drug must have the ability to retard the growth of pre-established metastatic colonies. We therefore employed an assay in which experimental metastases were established in the lungs of immune-compromised mice following tail-vein injection of Dunning rat AT6.1 prostate carcinoma. Drug treatment was begun only after colonies were visible in the lungs of test mice, generally at 5 days post-inoculation (Supplementary Fig. 1A). Mice were given intraperitoneal injections of vehicle or drugs in several doses, three times a week until signs of morbidity were observed. The drugs were first solubilized in DMSO and diluted with saline prior to injection. The dose selection was based on published studies using these agents in rodent experiments. The Kaplan-Meier survival curves of mice treated with fenbendazole, fluspirilene, suloctidil, clofazimine and niclosamide as well as the mean survival days of each group were shown in Figure 2. Except for fenbendazole at 250 mg/kg, all drugs showed little to moderate effect in improving the survival of mice. Compared to the vehicle-treated group (mean 30.6 days, 95% CI=29.1 to 33.1), mice receiving

fenbendazole treatment showed a significant increase of survival times (mean 36.9 days, 95% CI=35.4 to 38.4; P=0.04) (Fig. 2A). Fluspirilene at a lower dose (10 mg/kg) demonstrated a greater survival (mean 51.1 days, 95% CI=39.6 to 62.6 days vs. control mean 44.8 days, 95% CI=37.4 to 52.2 days) when compared to those with higher doses (20-40 mg/kg), suggesting that lower doses than 10 mg/kg may provide even greater survival benefit to these tumor-bearing mice (Fig. 2B).

Improved drug solubility for delivering anti-tumor agents in vivo

We observed that these drugs (except for suloctidil) are highly hydrophobic and produce visible aggregates when diluted with saline. Because these aggregates can be observed in the peritoneum of treated mice during autopsy, we hypothesize that low drug delivery to metastatic lesions in the lung may explain the lack of anti-tumor activity observed in the animal studies. To improve the solubility and systemic delivery of these agents, we determined that a combination of organic solvents including dimethyl sulfoxide (DMSO) and N-methyl-2-pyrrolidone (NMP) with surfactants Tween-80 and Cremophor EL (DNTC) in a 1:3:2:2 ratio provided improved solubility. This new vehicle did not cause significant toxicity to cultured cells (Fig. 3A). Moreover, fenbendazole solubilized in DNTC showed increased cytotoxicity for PC-3M and PC-3MLN4 prostate cancer cells compared to those solubilized in DMSO (Fig. 3A). There was ~2-fold reduction in ED50 (defined as the dose that kills 50% of the cell population) when tested in these cells (DMSO vs. DNTC, 5.5 μM (95% CI=5.3 to 5.7) vs. 2.76 μM (95% CI=2.6 to 2.9) in PC-3M and 2.1 μM (95% CI=2.05 to 2.15) vs. 1.1 μM (95% CI=1.03 to 1.17) in PC-3MLN4 cells, P<0.0001) (Fig. 3B).

To further evaluate the use of the DNTC as a vehicle in vivo, we determined the

bioavailability of this formulation by measuring the plasma level of fenbendazole and its active metabolites, fenbendazole sulfone and sulfoxide. Mice were injected intraperitoneally with a bolus dose of fenbendazole, formulated either in DNTC or DMSO, at 50 and 150 mg/kg (Fig. 3C). At 8 hours post injection, plasma samples were collected and subjected to high performance liquid chromatography (HPLC) analysis. At both 50 and 150 mg/kg doses, the DNTC formulation provided greater than 10-fold increase in the level of fenbendazole metabolites detected in the plasma, when compared to the DMSO formulation, indicative of increased systemic drug absorption. Such increased plasma concentration should provide increased availability of these drugs to metastatic sites. To further test whether this is the case, we treated AT6.1 lung metastasis bearing mice with fenbendazole solubilized either in DMSO or in DNTC. As shown in Fig. 3D and E, we observed a greater anti-tumor activity of the drug in extending the survival of mice when solubilized in DNTC (DMSO-FBZ vs. DNTC-FBZ, mean survival days, 40.25 days (95% CI=39.5 to 41.0 days) vs. 50.75 days (95% CI=48.4 to 53.1 days), P<0.01). These data strongly suggest that improved solubility improves the anti-metastatic activity of these hydrophobic agents. In fact, the solubility of all other lead drugs including fluspirilene and clofazimine were greatly improved using this improvised vehicle, with the exception of niclosamide.

Selective anti-tumor activity of lead drugs in metastatic prostate cancer cells in vitro

We further compared the differential cytotoxicity observed with our lead drugs in both highly metastatic PC-3MLN4 and AT6.1 cells relative to the less aggressive PC-3M cells. We utilized DNTC formulation for fenbendazole, fluspirilene and clofazimine, and DMSO for suloctidil and niclosamide. All drugs tested showed greater cytotoxicity (lower ED50) for highly

metastatic PC-3MLN4 cells than in PC-3M cells (Fig. 4A). Except for clofazimine and fluspirilene, similar conclusion could also be made when comparing PC-3M with AT6.1 cells. The differential cytotoxicity observed with PC-3M and PC-3MLN4 cells correlates with drug-induced apoptosis, as indicated by annexin V staining for both early and late apoptosis (Fig. 4B). Greater apoptosis was observed in treated-PC-3MLN4 than in -PC-3M cells; these effects were significantly reduced after treatment with the caspase-3 inhibitor (z-VAD-FMK) (Fig. 4C).

To evaluate the selective cytotoxicity effects in vivo, we implanted PC-3M and PC-3MLN4 subcutaneously in nude mice, waited 14 days and then began treatment with fenbendazole (100 mg/kg, solubilized in DNTC) three times a week for five weeks. Fenbendazole treatment resulted in 44.9% tumor volume reduction in PC-3MLN4 tumors (vehicle vs. fenbendazole, 537.1% growth (95% CI=504.3 to 569.9%) vs. 296% growth (95% CI=271.21 to 320.79)), compared to 16.3% reduction in PC-3M tumors (vehicle vs. fenbendazole, 515% growth (95% CI=489 to 541%) vs. 431% growth (95% CI=404 to 457)) (Fig. 4D) ($P<0.005$). In addition, we also treated mice bearing Dunning rat AT6.1 lung metastases expressing secreted Gaussia luciferase with fenbendazole for two weeks. Using measurement of plasma luciferase activity as an indicator of overall tumor burden, we observed a significant reduction of tumor burden (vehicle vs. fenbendazole, mean 165.0 RLU (95% CI=136.9 to 193.1) vs. mean 63.76 (95% CI=52.82 to 74.7), $P<0.001$) (Fig. 4E). Consistently, immunohistochemical analysis of the lungs revealed a reduced Ki67 staining (vehicle vs. fenbendazole, Ki67 labeling index 132.1 (95% CI=142.8 to 143.34) vs. 131.7 (95% CI=131.45 to 131.89), $P<0.0001$) and increased caspase-3 staining (vehicle vs. fenbendazole, apoptotic index 1.35 (95% CI=0.94 to 1.76) vs. 18.4 (95% CI=18.19 to 18.69), $P<0.0001$), indicative of reduced cell proliferation and increased apoptosis in the treated tumors (Fig. 4F-G).

Effects of lead agents in paclitaxel-resistant prostate cancer cells

Men with metastatic prostate lesions who fail hormone deprivation therapy frequently undergo paclitaxel-based chemotherapy; however, they often succumb within months as a result of taxane resistance (6). Paclitaxel-resistant prostate cancer cells (PC-3TxR and DU-145TxR) (15) responded to fenbendazole in a dose dependent manner, but were refractory to paclitaxel treatment (Fig. 5A). In fact, fenbendazole, fluspirilene and suloctidil exhibited higher potency in the paclitaxel-resistant PC-3TxR cells than in the parental PC-3 cells, as evidenced by a lower ED50 (Fig. 6B). Interestingly, only fenbendazole demonstrated higher potency in paclitaxel-resistant DU-145TxR when compared to DU-145 cell (Fig. 6B). The observed cytotoxic activity correlated with the percent apoptosis induced in these cells (Fig. 6C). Anti-tumor activity was further confirmed in vivo in a subcutaneous PC-3TxR tumor model. When the tumors reached ~100 mm^3 in size, the mice were treated with paclitaxel (10 mg/kg) or fenbendazole (100 mg/kg in DNTC formulation) three times per week for three weeks. Consistent with our observation in vitro, the growth of paclitaxel-treated PC-3TxR tumors (mean 872.5 mm^3, 95% CI=811.7 to 933.3 mm^3) was significantly greater when compared to the control group (mean 421.7 mm^3, 95% CI=371.8 to 471.6 mm^3, P=0.002) (Fig. 6D and E). In contrast, fenbendazole-treated tumors remained small (mean 163 mm^3, 95% CI=146.9 to 179.1 mm^3, P=0.006) throughout the study (Fig. 6D and E).

Anti-tumor activity of albendazole against paclitaxel and metastatic bone lesion of prostate cancer

Among the five lead drugs identified from the in vitro screen, fenbendazole appears to possess a distinct anti-tumor activity against various properties of metastatic prostate cancer

cells. Since the aim of this study is to develop novel therapeutic agents for prostate cancer

patients with metastatic disease and fenbendazole is not currently used in human, we decided to

investigate the effects of albendazole, another anti-helminth benzimidazole compound. Like

fenbendazole, albendazole shares similar mechanism of action and it has been widely used to

treat various parasite infestations in humans (28). Interestingly, albendazole also demonstrates

greater cytotoxicity in highly metastatic PC-3MLN4 and AT6.1 prostate cancer cells when

compared to PC-3M cells, as shown with lower ED50 and higher induction of apoptosis

(Supplementary Fig. 2A-B). Similarly, albendazole retain anti-tumor activity against both

paclitaxel-resistant PC-3TxR and DU-145TxR cells (Supplementary Fig. 2C), suggesting

potential use of this agent in men with metastatic prostate cancer. In previous human studies,

albendazole has been delivered in its native insoluble form. In order to improve the delivery of

this agent in vivo, we utilized the DNTC formulation and were able to enhance the

bioavailability of albendazole in mice (Supplementary Fig. 2D).

We next compared the anti-tumor activity of albendazole with paclitaxel, a standard

chemotherapy regimen for men with metastatic prostate cancer. In the AT6.1 model described

above, we determined that paclitaxel at 10 mg/kg (three times a week) was the optimal dose to

provide extended survival with minimal toxicity (Supplementary Fig. 3). Both paclitaxel- and

albendazole-treated mice showed increased survival relative to the vehicle-treated group (mean

survival days, vehicle: 26.3 days (95% CI=25.6 to 27.2 days), paclitaxel: 34.3 days (95%

CI=33.2 to 35.2 days) (P=0.002), albendazole 100 mg/kg: 38.2 days (95% CI=37.3 to 39.1 days)

(P<0.0001) (Fig. 6A-B). There was no significant difference in survival advantage between

paclitaxel and albendazole 100 mg/kg. However, the increased survival provided by albendazole

at 250 mg/kg (mean survival days, 41 days (95% CI=40.2 to 41.8 days) was significantly greater

than that seen in paclitaxel group at its optimal dose of 10 mg/kg (P=0.008) (Fig. 6A-B).

We further investigated the effects of albendazole in a model of experimental bone colonization by injecting luciferase-expressing PC-3MLN4 cells directly into mouse tibia. Mice with confirmed bone lesions (as monitored by bioluminescent imaging) were treated with 100 mg/kg albendazole for two weeks. The albendazole-treated group showed reduced intraosseous tumor growth compared to the control (Fig. 6C), with a significant difference in average luciferase signal over the course of treatment (vehicle vs. ABZ, normalized RLU at day 15, 473.8 RLU (95% CI=390.1 to 55.8 RLU) vs. 111.5 RLU (95% CI=79.6 to 149.3 RLU) (P=0.008) (Fig. 6D). X-ray and micro-computed tomography (CT) imaging showed that vehicle-treated mice had extensive osteolysis due to the osteoclastic activity of PC-3MLN4 cells (29), whereas bone integrity was maintained in albendazole-treated mice (Fig. 6E, Supplementary Fig. 4A-B). Immunohistochemical analysis of these bone lesions further showed a reduction of Ki-67 labeling index (vehicle vs. ABZ, mean 178.2 (95% CI=176.2 to 180.2) vs. mean 140.4 (95% CI=138.4 to 142.4) (P<0.0001) and an increase of apoptotic index (vehicle vs. ABZ, mean 24.9 (95% CI=24.0 to 25.9) vs. mean 41.2 (95% CI=29.1 to 33.3) (P=0.006) in the albendazole-treated group (Supplementary Fig. 4C-D). These results demonstrated that the anti-tumor effects of albendazole extend to tumors growing in intraosseous spaces.

In the therapeutic studies performed above, we may be able to deliver albendazole to metastatic lesions in mice using DNTC formulation via intraperitoneal administration. This approach, however, may not be feasible for use in humans due to use of organic solvents. To further our attempt to develop albendazole as a potential therapeutic agent in treating men with disseminated prostate cancer, we sought a new vehicle for its systemic administration. We tested a PLGA-based delivery method, which, to our knowledge, has not been previously reported.

Using this method, we further increased the cytotoxicity of albendazole in metastatic PC-3MLN4 as well as AT6.1 cells in vitro (Supplementary Fig. 5). When tested in the AT6.1 lung metastasis model, we observed a significant survival increase in the albendazole-treated group (mean survival days, 33.5 days (95% CI=30.5 to 36.5 days) relative to the vehicle-treated group (mean survival days, 23.1 days (95% CI=21.25 to 24.9 days) (P<0.001) (Fig. 6F-G). This observation is particularly intriguing as the albendazole dose used was noticeably lower than with DNTC, and there were no signs of vehicle-induced toxicity observed in treated mice (Supplementary Fig. 5).

To conclude, our studies strongly suggest that it is feasible to identify novel and effective therapeutic agents from a multi-stages, phenotype-based screening of known drugs, and through improvisation of the pre-existing pharmacological knowledge, we may be able to find immediate novel uses for these agents in treating metastatic prostate cancer.

DISCUSSION

Although it is well established that tumor metastasis is the principal cause of cancer mortality, screening for cancer drugs too rarely focuses on the treatment of established metastases. Drugs that are selected for their ability to repress growth of the primary tumor or for their ability to block the dissemination of metastatic colonies are often presumed to be active against established metastases. This is infrequently found to be the case when these agents are brought to clinical trial, where they are often employed in late stage patients. The current study was designed to interrogate whether drugs could be screened on the basis of increased cytotoxicity for highly metastatic prostate cancer cells relative to less metastatic cells. Our

results suggest that such a screen is feasible and show further that such drugs are effective at reducing metastatic tumor burden while prolonging the lives of these experimental animals.

This study reveals that certain drugs such as albendazole may be potent anti-cancer agents for the treatment of disseminated, advanced prostate cancers. Identification of these drugs resulted from a phenotypic (metastasis)-based in vitro screening of a library of marketed drugs. "Hits" from this screen exhibit greater cytotoxicity for two highly metastatic human prostate cancer cell lines relative to their less metastatic counterparts and minimal cytotoxicity on normal prostate epithelial cells. These agents were then screened in a stringent assay for a significant survival benefit in mice bearing pre-existing lung colonies of prostate cancer cells. Fenbendazole, in particular, demonstrated greater survival-promoting effects among other agents. Fenbendazole was also cytotoxic against paclitaxel-resistant prostate cancer, one of the major challenges in the clinic. Such anti-tumor effects were also extended to albendazole, a member in the family of benzimidazole compounds (30). Albendazole treatment was comparable, if not superior to, paclitaxel, a current front-line treatment for metastatic prostate cancer. We also demonstrate that albendazole was growth inhibitory to prostate cancer cells residing in lung or in bone.

The mechanism(s) by which these agents induced selective cytotoxicity on metastatic prostate cancer cells remains unclear. Fenbendazole and albendazole are used commonly in veterinary and human medicine as anti-parasitic and anti-fungal agents (31), mainly by inhibiting tubulin polymerization (32, 33). Although not widely utilized as anti-cancer drugs, they have shown anti-tumor activity for human cancer cell lines implanted in nude mice (33-35). Niclosamide is shown to uncouple oxidative phosphorylation processes in the tapeworm (36) by affecting signaling pathways in cancer cells (37, 38). Fluspirilene, a potent anti-psychotic drug,

acts by blocking Ca2+ channels (26, 39). While its anti-tumor activity is under-studied, it is

shown to promote autophagy in tumor cells without causing obvious cellular damage (40).

Clofazimine, a drug for treating leprosy and tuberculosis, has been investigated to treat colon,

liver and lung cancer (41-43). Studies showed that clofazimine inhibits cell proliferation by

inducing activity of phospholipid A2 (25, 44). Finally, suloctidil may affect cell proliferation by

inhibiting cyclo-oxygenase activity, although its reported mechanism of action as a vasodilator

involves inhibition of platelet aggregation (27). Further studies will be required to elucidate the

common mechanism(s) of action shared by these drugs (if any) in exhibiting preferential

cytotoxicity towards highly metastatic prostate cancer cells when compared to the poorly

metastatic cells.

Taxane-resistance has been a major clinical problem in the treatment of men with

metastatic prostate cancer (8), and we are in need of alternative therapeutic options for these

patients. In this study, we tested two different paclitaxel-resistant prostate cancer cells (PC-

3TxR and DU-145TxR) in comparison to their sensitive counterparts. Despite potent

cytotoxicity against metastatic prostate cancer cells, not all the lead agents identified from the

screen demonstrate similar activity towards paclitaxel-resistant cells. Only fenbendazole and

albendazole exhibited greater anti-tumor activity (as indicated by lower ED50) in both of PC-3

and DU-145 resistant cells relative to the parental cells. Although these agents work similarly as

paclitaxel by targeting the microtubule polymerization, benzimidazoles may represent an

alternative class of anti-cancer agents: 1) The tubulin-binding site of benzimidazoles is distinctly

different from those targeted by paclitaxel or vinblastine; benzimidazoles bind to sites located on

the outside of the microtubule while others bind near the intradimer interface facing the

microtubule lumen (45, 46); 2) Unlike most chemotherapeutic drugs, the active metabolites of

albendazole and fenbendazole are not substrates for the human breast cancer resistance protein (Bcrp1/ABCG2), multidrug resistant protein (MRP)2 or P-glycoprotein (Pgp) (47).

Despite identification of fenbendazole from our screen, we determined that this veterinary compound may not be as clinically applicable when compared to albendazole, another member of the same drug family. Albendazole is mainly given orally, and it is poorly absorbed from the gastrointestinal tract due to its low aqueous solubility (30). In order to treat metastatic lesion with albendazole, efficient systemic delivery is inevitable (necessary). Here, we provided the proof of principle evidence that improved bioavailability can lead to a greater anti-tumor activity in vivo. While DNTC vehicle may be applicable in experimental animals, we showed that an FDA-approved, biodegradable and biocompatible PLGA-PEG nanoparticle formulation may be as useful for clinical application in human (16, 48). Our studies suggest that albendazole, when solubilized in either the improvised DNTC or nanoparticle-based formulation, exhibited profound anti-tumor activity by reducing tumor burden in the lung as well as in the bone, which consequently lead to improvement of survival of these mice. More importantly, the dose range that showed potent anti-tumor effects in this study (low microMolar in vitro and 100 mg/kg in vivo) are within the achievable pharmacological levels in humans (28). Because of its relatively benign safety profile, it should be possible to use albendazole in the long term treatment of metastatic cancers, even in patients whose tumors have become resistant to other drugs (49). A small clinical trial of albendazole in patients with advanced hepatocellular carcinoma showed promising anti-tumor activity (stabilization of disease) and well-tolerated side effects (50).

In summary, our phenotypic-based screening platform allows for reprioritization of drugs that are active against highly metastatic tumor cells for further clinical development. As proof of

principle, we demonstrated that these drugs have profound anti-tumor activity against metastatic and taxane-resistant prostate cancer cells. Similar screens for anti-metastatic drugs should be feasible for other metastatic cancers and may reveal additional drug classes that can extend the lives of late-stage cancer patients.

FIGURE LEGENDS

Figure 1. Screen for agents with a selective cytotoxicity for highly metastatic prostate cancer cells.

(A) Diagram shows the results of a screen for cytotoxic agents against metastatic prostate cancer cells. 1120 drugs were tested in at least two concentrations. Fenbendazole exhibited: 1) greater cell kill in highly metastatic PC-3MLN4 compared to less metastatic PC-3M cells at 10 μM ($P<0.01$) (Screen I); 2) greater cell kill in both highly metastatic PC-3MLN4 and DU-145LN4 cells compared to the less metastatic counterparts (Screen II). $P<0.01$ for cell kill at 1 and 10 μM; 3) a greater than 40% cell kill in AT6.1 cells (Screen III) ($P<0.001$ for dose above 0.1 μM; and 4) minimal cytotoxicity in normal prostate epithelial nBE cells (Screen IV) ($P>0.05$). (B) Representative dose response testing fenbendazole on prostate cancer and normal prostate cells for 48 hours. Data shown are mean ± 95% confidence interval, N=4 per group.

Figure 2. In vivo screening of the five lead hits in survival assay of disseminated Dunning rat AT6.1 prostate carcinoma cells.

To generate pre-existing micrometastatic lesions, AT6.1 Dunning rat prostate carcinoma cells were injected intravenously into nude mice five days prior to treatment. Fenbendazole (A), flusprilene (B), suloctidil (C), clofazimine (D) and niclosamide (E) were given three times a

week via intraperitoneal injection until signs of morbidity was observed. The drugs were solubilized in DMSO and diluted with saline prior to injection. Shown is Kaplan-Meier survivals curves (left) and mean survival (right) of mice treated with either vehicle (control) or agents. Data shown are mean ± 95% confidence interval, N=10 per group.

Figure 3. Enhanced anti-tumor activity of fenbendazole was observed upon improvement in solubility and bioavailability.

(A) Fenbendazole (FBZ) cytotoxicity in PC-3MLN4 cells is shown for drugs solubilized in either DNTC or DMSO. DNTC itself exhibits minimal cytotoxicity. (B) Comparison of ED50 of fenbendazole (FBZ) when formulated in the two different vehicles, DMSO and DNTC. (C) Measurement of FBZ and its active metabolites (FBZSO and $FBZSO_2$) in the mouse plasma collected after one injection. FBZ was not detected in all samples. *, under limit of detection. (D) AT6.1 cells were inoculated intravenously 5 days prior to treatment of 100 mg/kg fenbendazole either in DMSO or DNTC, given 3 times a week until signs of morbidity were observed. Shown are Kaplan Meier survival curve of mice in each group. (E) Average of survival days for each treatment group from (D). Data shown are mean ± 95% confidence interval, N=10 per group.

Figure 4. Selective anti-tumor activity of lead hits on highly aggressive, metastatic prostate cancer cells.

(A) ED50 of agents for highly metastatic (PC-3MLN4 and AT6.1) and less metastatic (PC-3M) prostate cancer cells after 72 hr treatment, as determined using Cyquant proliferation assay. Data shown are mean ± 95% confidence interval, N=3 per group. (B) Percent apoptosis was

determined by annexin V-stained cells after 72 hr treatment with 1 μM drug. Data shown are mean ± 95% confidence interval, N=4 per group. (C) Drug-induced apoptosis in PC-3MLN4 was greatly reduced by treatment with 20 μM caspase-3 inhibitor (Z-VAD-FMK). (D) PC-3M and PC-3MLN4 subcutaneous tumors were treated with 100 mg/kg fenbendazole, three times a week for five weeks. Percent tumor growth was calculated from the tumor volume measured on first day of treatment. Data shown are mean ± 95% confidence interval, N=10 per group. (E-G) AT6.1 cells were inoculated via tail vein 5 days prior to treatment with 100 mg/kg fenbendazole, given 3 times a week until day 22 when signs of morbidity were observed in the control group. (E) Secreted Gaussia luciferase activity in the peripheral blood, indicative of tumor burden in the mice was measured on the day of harvest. (F) Representative staining of Ki-67 and activated caspase-3 on tumors in the lungs. (G) Ki-67 labeling and apoptotic index was determined using Imagescope software (Aperio). N=10 mice/group, *, P<0.005.

Figure 5. Effects of lead agents in paclitaxel-resistant prostate cancer cells.
(A) Cytotoxic effects of paclitaxel and fenbendazole (FBZ) in paclitaxel-resistant prostate cancer cells. (B) Comparison of ED50 of agents in paclitaxel-sensitive and –resistant cell lines. (C) Percent apoptosis induced by each agent in paclitaxel-sensitive and –resistant cell lines, as measured by annexin V staining. (D) Relative growth of subcutaneous PC-3TxR tumors after treatment with DNTC alone, paclitaxel or FBZ in DNTC. Treatment was given three times per week for three weeks. (E) Average of tumor size from each treatment group at the end of study. Data shown are mean ± 95% confidence interval, N=10 per group.

Figure 6. Anti-tumor activity of albendazole in comparison with paclitaxel and in experimental bone metastasis of prostate cancer in vivo.

(A-B) AT6.1 cells were inoculated intravenously five days prior to treatment of either paclitaxel or albendazole (ABZ). Shown are Kaplan Meier survival curve (A) and the average survival days (B) for each treatment group. (C-E) Bone lesions of PC-3MLN4 cells were generated by intraosseous injection into the tibia of mice, before treatment with vehicle or 100 mg/kg albendazole (ABZ), three times a week for two weeks. (C) Representative photos of luciferase signal detected in each treatment group at the beginning and end of study. (D) Mean of luciferase signals detected in mice during the course of treatment, as a measurement of tumor burden. (E) Representative images from X-ray (left) and micro-CT (right) analysis showing differences in radiographical characteristics of the bone lesions. Data shown are mean ± 95% confidence interval, N=10 per group.

REFERENCES

1.   Jemal A, Siegel R, Xu J, Ward E. Cancer statistics, 2010. CA Cancer J Clin;60(5):277-300.

2.   Kupelian PA, Elshaikh M, Reddy CA, Zippe C, Klein EA. Comparison of the efficacy of local therapies for localized prostate cancer in the prostate-specific antigen era: a large single-institution experience with radical prostatectomy and external-beam radiotherapy. J Clin Oncol 2002;20(16):3376-85.

3.   Coen JJ, Zietman AL, Thakral H, Shipley WU. Radical radiation for localized prostate cancer: local persistence of disease results in a late wave of metastases. J Clin Oncol 2002;20(15):3199-205.

4.   Bhandari MS, Petrylak DP, Hussain M. Clinical trials in metastatic prostate cancer--has there been real progress in the past decade? Eur J Cancer 2005;41(6):941-53.

5.   Petrylak DP. Chemotherapy for androgen-independent prostate cancer. Semin Urol Oncol 2002;20(3 Suppl 1):31-5.

6.   Tannock IF, de Wit R, Berry WR, Horti J, Pluzanska A, Chi KN, et al. Docetaxel plus prednisone or mitoxantrone plus prednisone for advanced prostate cancer. N Engl J Med 2004;351(15):1502-12.

7.   Petrylak DP. The treatment of hormone-refractory prostate cancer: docetaxel and beyond. Rev Urol 2006;8 Suppl 2:S48-55.

8.   Mancuso A, Oudard S, Sternberg CN. Effective chemotherapy for hormone-refractory prostate cancer (HRPC): present status and perspectives with taxane-based treatments. Crit Rev Oncol Hematol 2007;61(2):176-85.

9.   Mani SA, Guo W, Liao MJ, Eaton EN, Ayyanan A, Zhou AY, et al. The epithelial-mesenchymal transition generates cells with properties of stem cells. Cell 2008;133(4):704-15.

10.   Zhau HE, He H, Wang CY, Zayzafoon M, Morrissey CM, Vessella RL, et al. Human prostate cancer harbors the stem cell properties of bone marrow mesenchymal stem cells. Clin Cancer Res.

11.   Keysar SB, Jimeno A. More than markers: biological significance of cancer stem cell-defining molecules. Mol Cancer Ther;9(9):2450-7.

12.   Everley PA, Krijgsveld J, Zetter BR, Gygi SP. Quantitative cancer proteomics: stable isotope labeling with amino acids in cell culture (SILAC) as a tool for prostate cancer research. Mol Cell Proteomics 2004;3(7):729-35.

13.   Pettaway CA, Pathak S, Greene G, Ramirez E, Wilson MR, Killion JJ, et al. Selection of highly metastatic variants of different human prostatic carcinomas using orthotopic implantation in nude mice. Clin Cancer Res 1996;2(9):1627-36.

14.   Chung LW, Chang SM, Bell C, Zhau HE, Ro JY, von Eschenbach AC. Co-inoculation of tumorigenic rat prostate mesenchymal cells with non-tumorigenic epithelial cells results in the development of carcinosarcoma in syngeneic and athymic animals. Int J Cancer 1989;43(6):1179-87.

15.   Takeda M, Mizokami A, Mamiya K, Li YQ, Zhang J, Keller ET, et al. The establishment of two paclitaxel-resistant prostate cancer cell lines and the mechanisms of paclitaxel resistance with two cell lines. Prostate 2007;67(9):955-67.

16.   Sengupta S, Eavarone D, Capila I, Zhao G, Watson N, Kiziltepe T, et al. Temporal targeting of tumour cells and neovasculature with a nanoscale delivery system. Nature 2005;436(7050):568-72.

17.   Feng YH, Li X, Wang L, Zhou L, Gorodeski GI. A truncated P2X7 receptor variant (P2X7-j) endogenously expressed in cervical cancer cells antagonizes the full-length P2X7 receptor through hetero-oligomerization. J Biol Chem 2006;281(25):17228-37.

18.   Chou TC. Preclinical versus clinical drug combination studies. Leuk Lymphoma 2008;49(11):2059-80.

19.   Berlin O, Samid D, Donthineni-Rao R, Akeson W, Amiel D, Woods VL, Jr. Development of a novel spontaneous metastasis model of human osteosarcoma transplanted orthotopically into bone of athymic mice. Cancer Res 1993;53(20):4890-5.

20.   Wurdinger T, Badr C, Pike L, de Kleine R, Weissleder R, Breakefield XO, et al. A secreted luciferase for ex vivo monitoring of in vivo processes. Nat Methods 2008;5(2):171-3.

21.   Isaacs JT, Isaacs WB, Feitz WF, Scheres J. Establishment and characterization of seven Dunning rat prostatic cancer cell lines and their use in developing methods for predicting metastatic abilities of prostatic cancers. Prostate 1986;9(3):261-81.

22.   Dong JT, Lamb PW, Rinker-Schaeffer CW, Vukanovic J, Ichikawa T, Isaacs JT, et al. KAI1, a metastasis suppressor gene for prostate cancer on human chromosome 11p11.2. Science 1995;268(5212):884-6.

23.   Villar D, Cray C, Zaias J, Altman NH. Biologic effects of fenbendazole in rats and mice: a review. J Am Assoc Lab Anim Sci 2007;46(6):8-15.

24.   Tanowitz HB, Weiss LM, Wittner M. Diagnosis and treatment of intestinal helminths. I. Common intestinal cestodes. Gastroenterologist 1993;1(4):265-73.

25.   Arbiser JL, Moschella SL. Clofazimine: a review of its medical uses and mechanisms of action. J Am Acad Dermatol 1995;32(2 Pt 1):241-7.

26.   Janssen PA, Niemegeers CJ, Schellekens KH, Lenaerts FM, Verbruggen FJ, van Nueten JM, et al. The pharmacology of fluspirilene (R 6218), a potent, long-acting and injectable neuroleptic drug. Arzneimittelforschung 1970;20(11):1689-98.

27.   Bucchi F, Cerletti C, de Gaetano G. Inhibition of platelet thromboxane generation by suloctidil in man. Haemostasis 1986;16(5):362-8.

28.   Takayanagui OM, Lanchote VL, Marques MP, Bonato PS. Therapy for neurocysticercosis: pharmacokinetic interaction of albendazole sulfoxide with dexamethasone. Ther Drug Monit 1997;19(1):51-5.

29.   Singh AS, Figg WD. In vivo models of prostate cancer metastasis to bone. J Urol 2005;174(3):820-6.

30.   Marriner SE, Morris DL, Dickson B, Bogan JA. Pharmacokinetics of albendazole in man. Eur J Clin Pharmacol 1986;30(6):705-8.

31.   Lanusse CE, Prichard RK. Clinical pharmacokinetics and metabolism of benzimidazole anthelmintics in ruminants. Drug Metab Rev 1993;25(3):235-79.

32.   Lacey E. Mode of action of benzimidazoles. Parasitol Today 1990;6(4):112-5.

33.   Pourgholami MH, Woon L, Almajd R, Akhter J, Bowery P, Morris DL. In vitro and in vivo suppression of growth of hepatocellular carcinoma cells by albendazole. Cancer Lett 2001;165(1):43-9.

34.   Pourgholami MH, Akhter J, Wang L, Lu Y, Morris DL. Antitumor activity of albendazole against the human colorectal cancer cell line HT-29: in vitro and in a xenograft model of peritoneal carcinomatosis. Cancer Chemother Pharmacol 2005;55(5):425-32.

35.   Pourgholami MH, Yan Cai Z, Lu Y, Wang L, Morris DL. Albendazole: a potent inhibitor of vascular endothelial growth factor and malignant ascites formation in OVCAR-3 tumor-bearing nude mice. Clin Cancer Res 2006;12(6):1928-35.

36.   Weinbach EC, Garbus J. Mechanism of action of reagents that uncouple oxidative phosphorylation. Nature 1969;221(5185):1016-8.

37.   Jin Y, Lu Z, Ding K, Li J, Du X, Chen C, et al. Antineoplastic mechanisms of niclosamide in acute myelogenous leukemia stem cells: inactivation of the NF-kappaB pathway and generation of reactive oxygen species. Cancer Res;70(6):2516-27.

38.   Wang AM, Ku HH, Liang YC, Chen YC, Hwu YM, Yeh TS. The autonomous notch signal pathway is activated by baicalin and baicalein but is suppressed by niclosamide in K562 cells. J Cell Biochem 2009;106(4):682-92.

39.   Enyeart JJ, Biagi BA, Day RN, Sheu SS, Maurer RA. Blockade of low and high threshold Ca2+ channels by diphenylbutylpiperidine antipsychotics linked to inhibition of prolactin gene expression. J Biol Chem 1990;265(27):16373-9.

40.   Zhang L, Yu J, Pan H, Hu P, Hao Y, Cai W, et al. Small molecule regulators of autophagy identified by an image-based high-throughput screen. Proc Natl Acad Sci U S A 2007;104(48):19023-8.

41.   Falkson CI, Falkson G. A phase II evaluation of clofazimine plus doxorubicin in advanced, unresectable primary hepatocellular carcinoma. Oncology 1999;57(3):232-5.

42.   Ruff P, Chasen MR, Long JE, van Rensburg CE. A phase II study of oral clofazimine in unresectable and metastatic hepatocellular carcinoma. Ann Oncol 1998;9(2):217-9.

43.   Sri-Pathmanathan RM, Plumb JA, Fearon KC. Clofazimine alters the energy metabolism and inhibits the growth rate of a human lung-cancer cell line in vitro and in vivo. Int J Cancer 1994;56(6):900-5.

44.   Van Rensburg CE, Van Staden AM, Anderson R. The riminophenazine agents clofazimine and B669 inhibit the proliferation of cancer cell lines in vitro by phospholipase A2-mediated oxidative and nonoxidative mechanisms. Cancer Res 1993;53(2):318-23.

45.   Hamel E. Antimitotic natural products and their interactions with tubulin. Med Res Rev 1996;16(2):207-31.

46.   Downing KH. Structural basis for the interaction of tubulin with proteins and drugs that affect microtubule dynamics. Annu Rev Cell Dev Biol 2000;16:89-111.

47.   Merino G, Jonker JW, Wagenaar E, Pulido MM, Molina AJ, Alvarez AI, et al. Transport of anthelmintic benzimidazole drugs by breast cancer resistance protein (BCRP/ABCG2). Drug Metab Dispos 2005;33(5):614-8.

48.   Farokhzad OC, Cheng J, Teply BA, Sherifi I, Jon S, Kantoff PW, et al. Targeted

nanoparticle-aptamer bioconjugates for cancer chemotherapy in vivo. Proc Natl Acad Sci U S A

2006;103(16):6315-20.

49.   Vuitton DA. Benzimidazoles for the treatment of cystic and alveolar echinococcosis:

what is the consensus? Expert Rev Anti Infect Ther 2009;7(2):145-9.

50.   Morris DL, Jourdan JL, Pourgholami MH. Pilot study of albendazole in patients with

advanced malignancy. Effect on serum tumor markers/high incidence of neutropenia. Oncology

2001;61(1):42-6.

Figure 1

A

	Screen I	Screen II	Screen III	Screen IV
Cell system	PC-3MLN4 > PC-3M	PC-3MLN4 > PC-3M DU-145LN4 > DU-145	AT6.1	nBE
Dose	10 μM	0.1 - 10 μM	0.1 - 10 μM	0.1 - 10 μM
Total compounds	1120	44	23	10
Total hits (%)	44 (4%)	23 (2%)	10 (0.9%)	5 (0.44%)

B
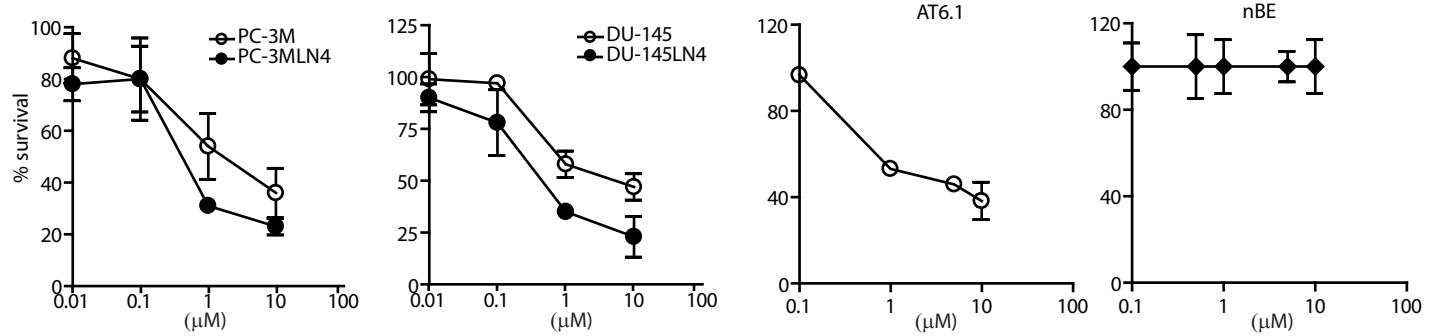
Figure 2

Figure 3

Figure 4

A

Compound	ED50 (μM)		
	PC-3M	PC-3MLN4	AT6.1
Clofazimine	10.78 (10.24 - 11.32)	8.49 (7.75 - 9.23)	15.2 (13.87 - 16.53)
Fenbendazole	1.37 (1.08 - 1.64)	0.67 (0.58 - 0.76)	0.95 (0.85 - 1.05)
Fluspirilene	15.10 (13.37 - 14.83)	9.07 (8.49 - 9.65)	31.6 (30.19 - 33.01)
Suloctidil	23.9 (22.6 - 25.2)	7.84 (7.18 - 8.50)	6.45 (5.84 - 7.06)
Niclosamide	1.62 (1.41 - 1.79)	0.44 (0.38 - 0.50)	1.59 (1.42 - 1.78)

Figure 5

A

B
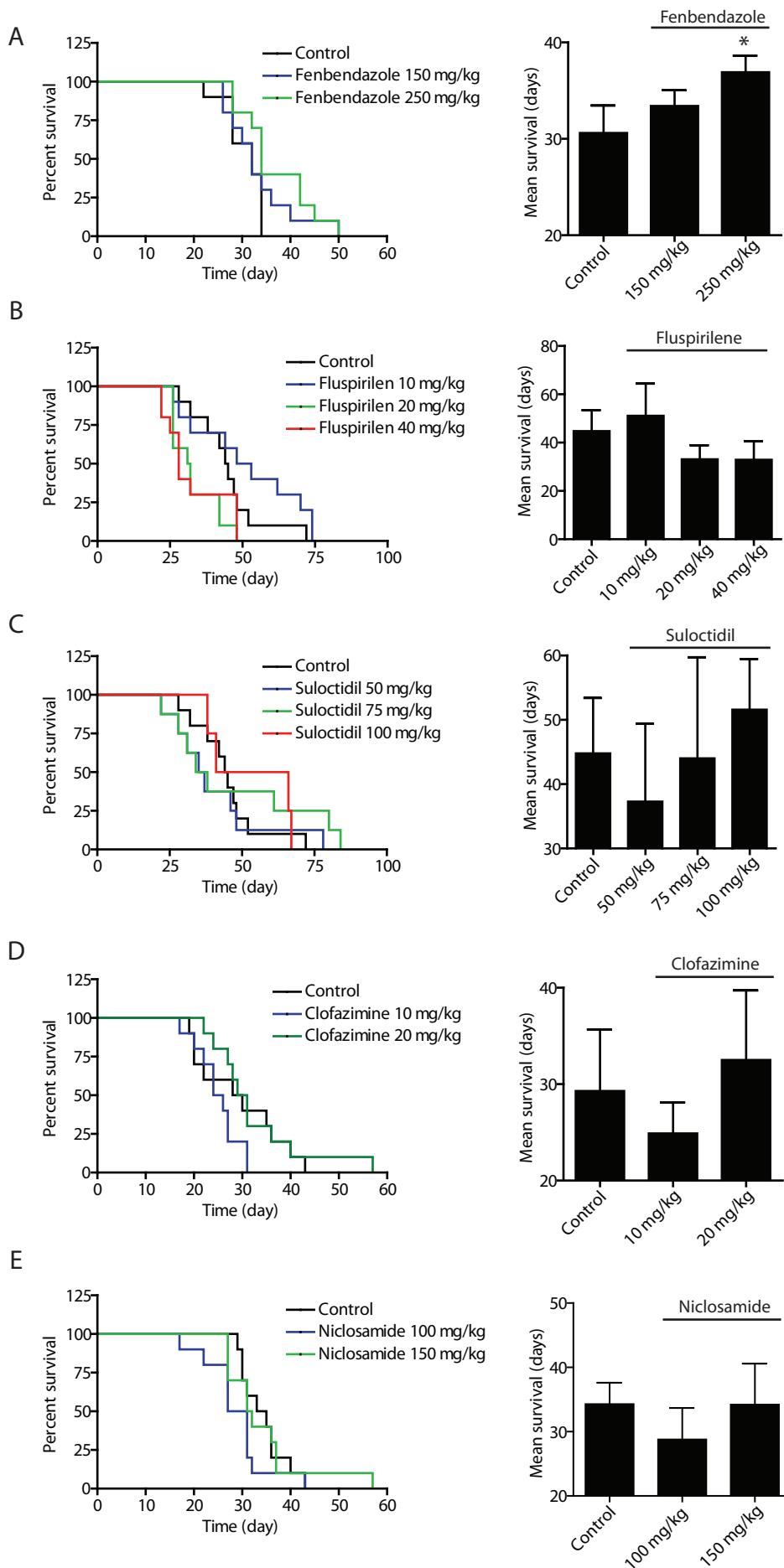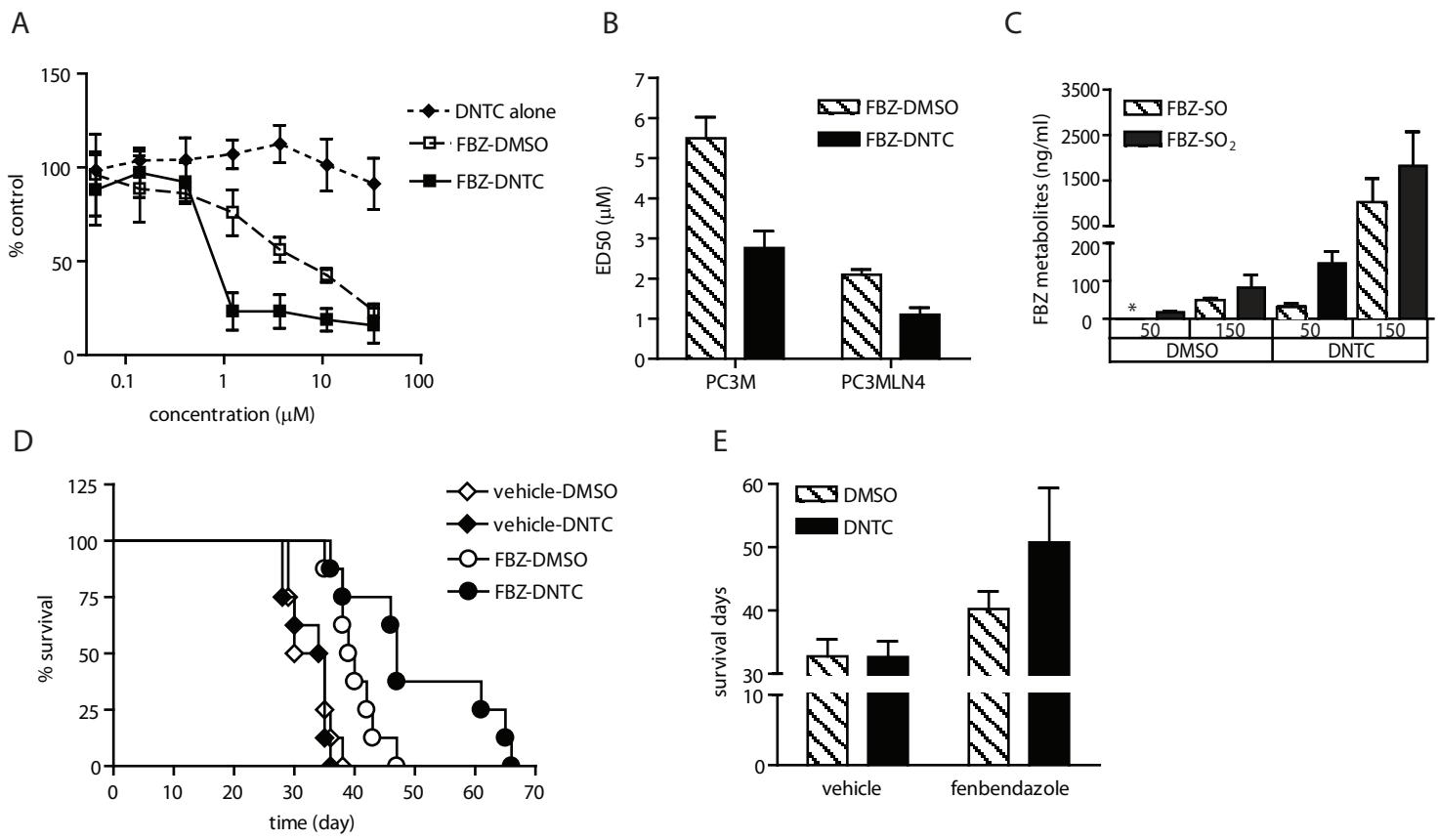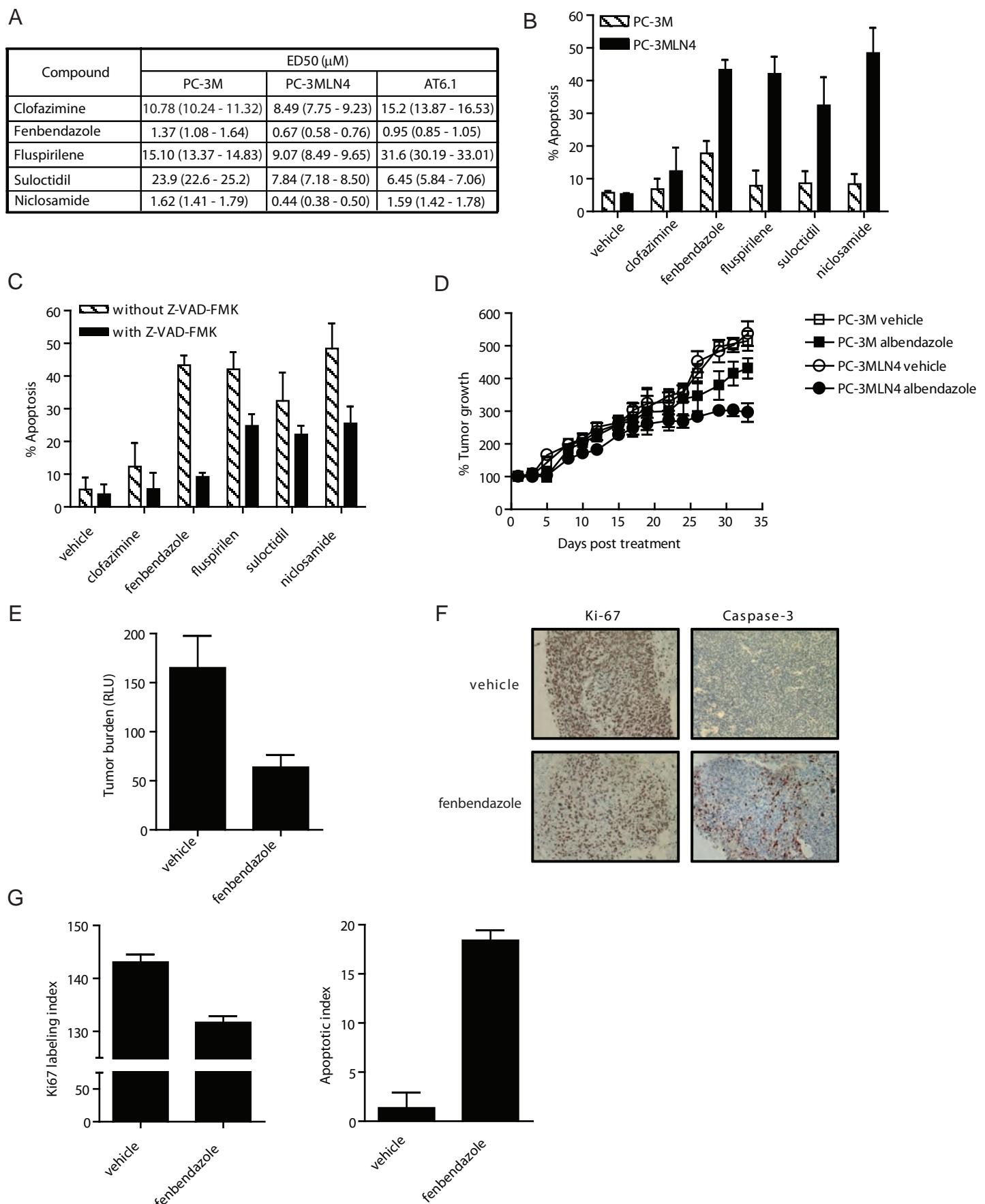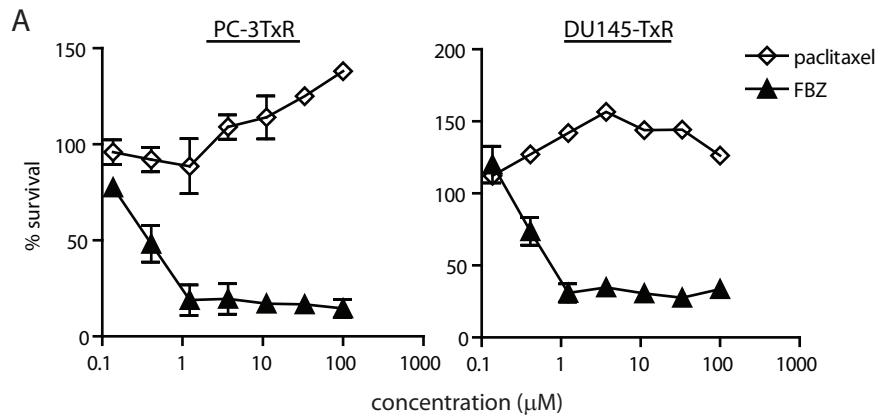
Compound	ED50 (µM)			
	PC3	PC-3TxR	DU145	DU145-TxR
Clofazimine	14.8 (14.3 - 15.2)	26.0 (25.1 - 27.0)	55.2 (50.1 - 60.3)	115 (102 - 127)
Fenbendazole	1.82 (1.51 - 2.12)	0.44 (0.32 - 0.58)	10.4 (9.8 - 10.9)	4.70 (4.18 - 5.22)
Fluspirilene	39.7 (38.1 - 41.2)	36.7 (35.1 - 38.4)	19.5 (18.7 - 20.3)	56.4 (54.9 - 57.8)
Suloctidil	30.8 (30.3 - 31.3)	27.1 (26.7 - 27.6)	6.88 (6.31 - 7.45)	23.8 (22.2 - 25.4)
Niclosamide	41.1 (40.5 - 41.6)	56.0 (53.9 - 58.1)	15.0 (14.3 - 15.7)	117 (114 - 120)

C

D

E
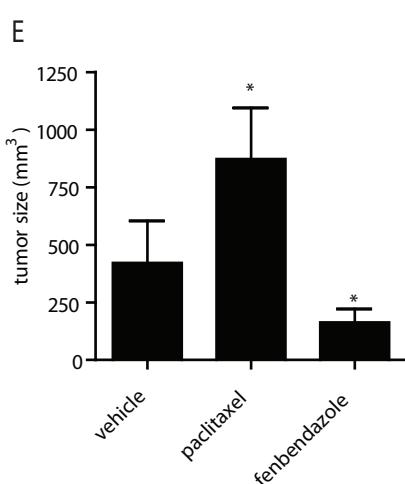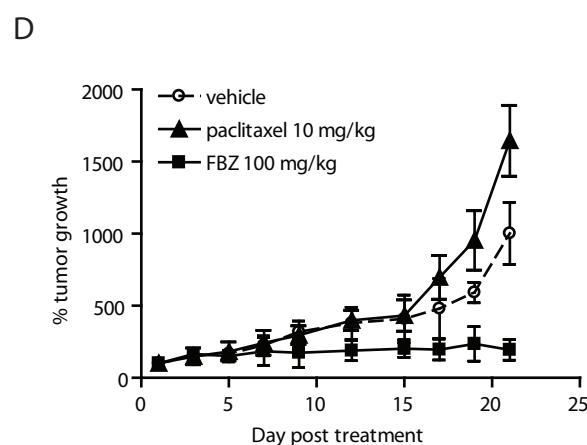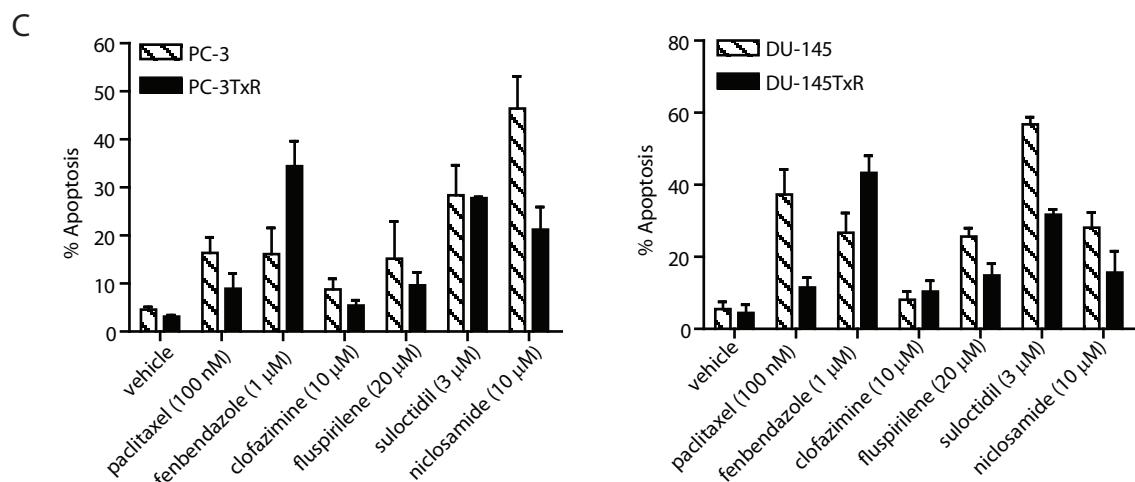
Figure 6
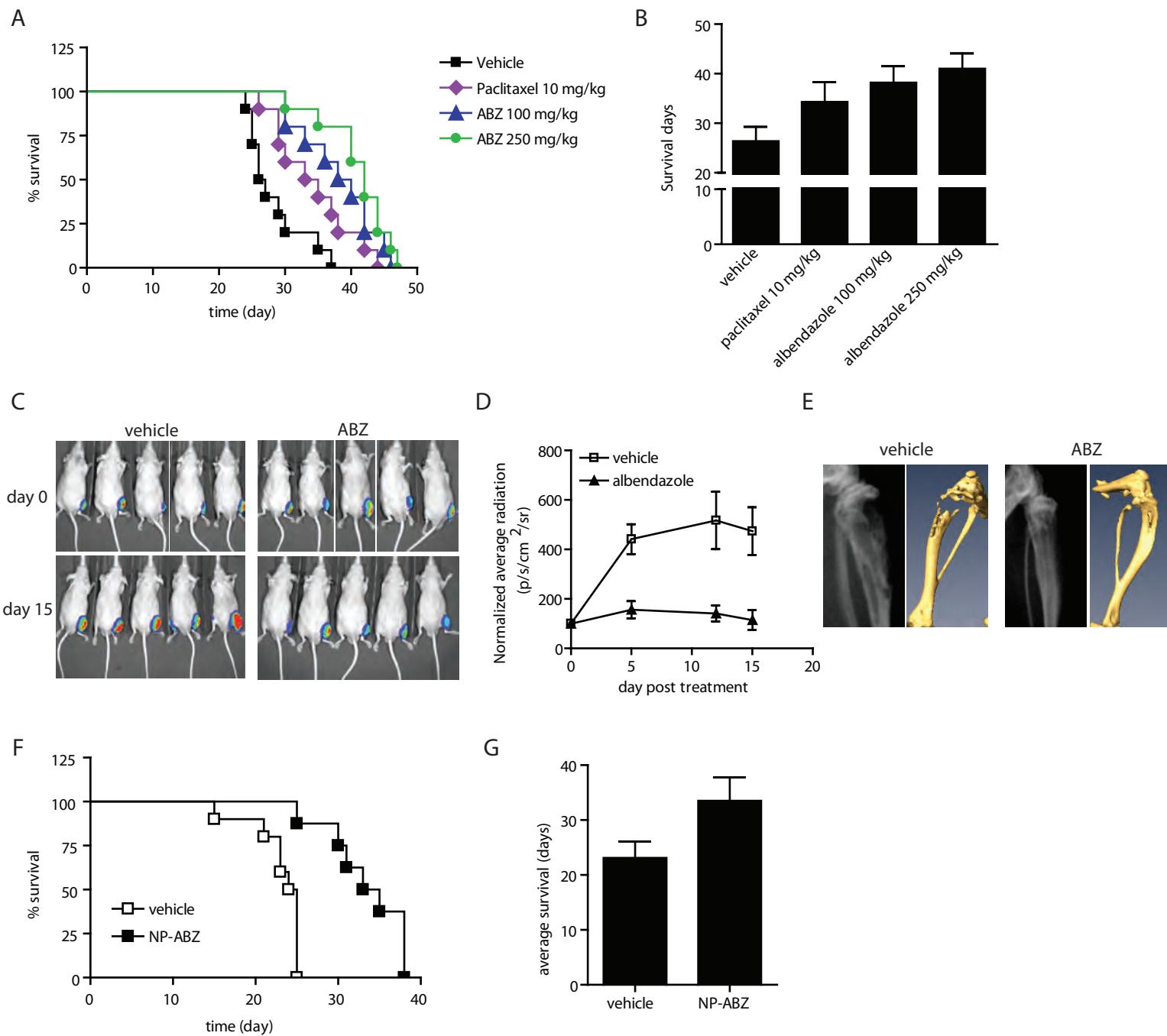
Fig. 7 Anti-tumor activity of albendazole in comparison with paclitaxel and in experimental bone metastasis of prostate cancer in vivo.

(A-B) AT6.1 cells were inoculated intravenously five days prior to treatment of either paclitaxel or albendazole (ABZ). Kaplan Meier survival curve (A) and the average survival days (B) for each treatment group; (C-E) Bone lesions of PC-3MLN4 cells were generated by intraosseous injection into the tibia of mice, before treatment with vehicle or 100 mg/kg albendazole (ABZ), three times a week for two weeks. (C) Representative photos of luciferase signal detected in each treatment group at the beginning and end of study; (D) Mean of luciferase signals detected in mice during the course of treatment, as a measurement of tumor burden; (E) Representative images from X-ray (left) and micro-CT (right) analysis showing differences in radiographical characteristics of the bone lesions;
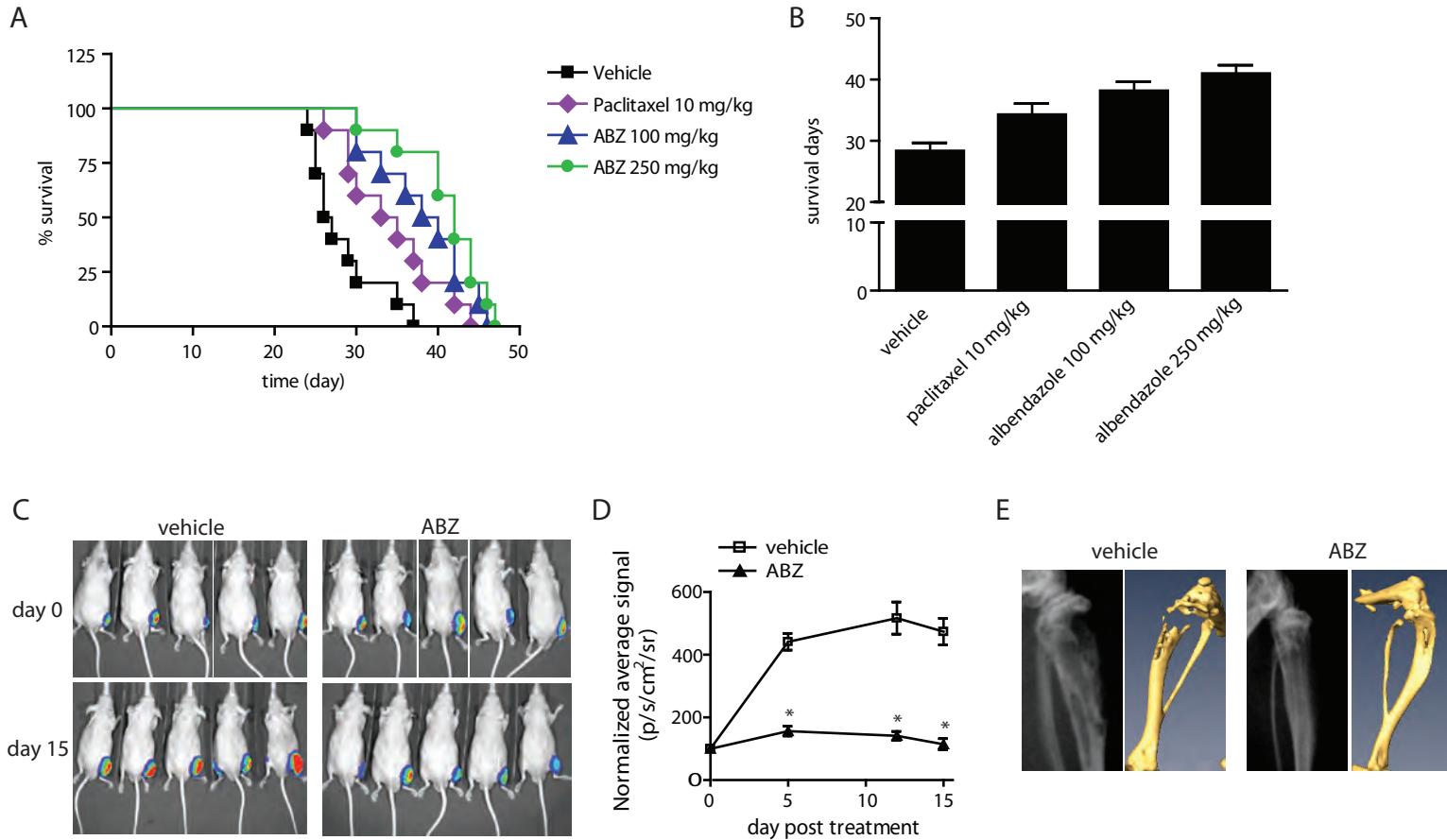
Sup. Figure 1: No changes in body weight of mice after treatment of fenbendazole.

Dunning rat prostate carcinoma AT6.1 cells were inoculated intravenously 5 days prior to treatment of fenbendazole (100 mg/kg), given 3 times a week for 21 days. Body weight of the mice were recorded over the course of treatment. N=10 per group.

A

B
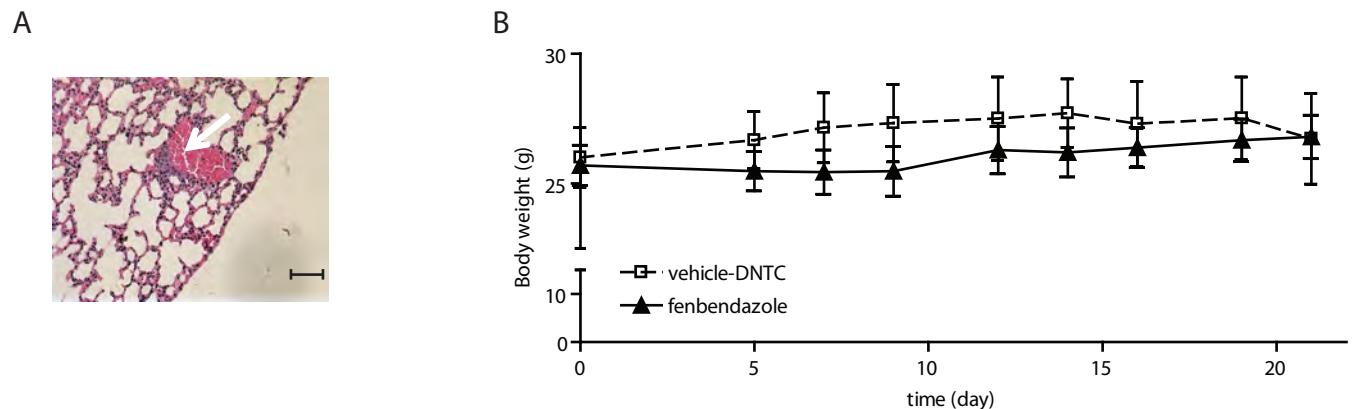
Supplementary Figure 2: Effects of albendazole on metastatic prostate cancer cells

(A) ED50 of albendazole for 72 hour treatment in highly metastatic PC-3MLN4 and AT6.1 cells relative to poorly metastatic PC-3M cells.

(B) Albendazole-induced apoptosis in PC-3M and PC-3MLN4 cells was measured using annexin V staining. Cells were treated either with vehicle or 1 μM albendazole for 72 hours before subjected for FACS analysis. In another experiment, cells were also treated with 20 μM Z-VAD-FMK caspase inhibitor concurrently.

(C) Dose response curves of paclitaxel-resistant PC-3TxR and DU-145TxR cells after 72 hours treatment with albendazole.

(D) Measurement of albendazole and its metabolites in mouse plasma. Albendazole dissolved in either DMSO or DNTC was given one time to the mice at 50 and 150 mg/kg. Plasma samples were prepared from whole blood from each mouse at 8 hr post injection. ABZ and its metabolites, ABZ-SO and ABZ-SO2 were measured using HPLC. N= 3 per group.
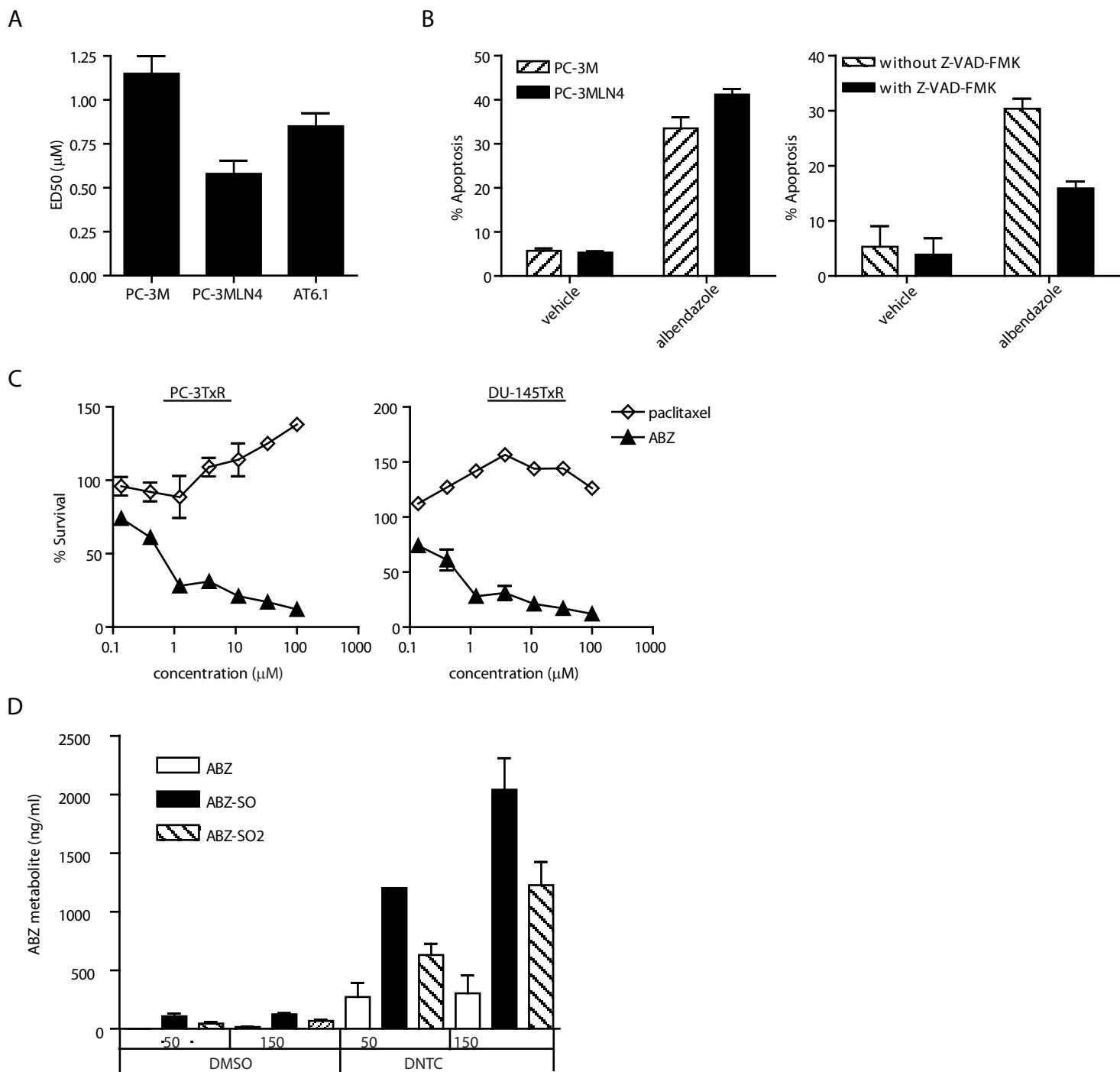
Supplementary Figure 3: Effects of fenbendazole and paclitaxel in AT6.1 intravenous lung metastasis model.

Dunning rat prostate carcinoma AT6.1 cells were inoculated intravenously 5 days prior to treatment of paclitaxel given 3 times a week until signs of morbidity were observed. N=10 per group. *, P<0.01.
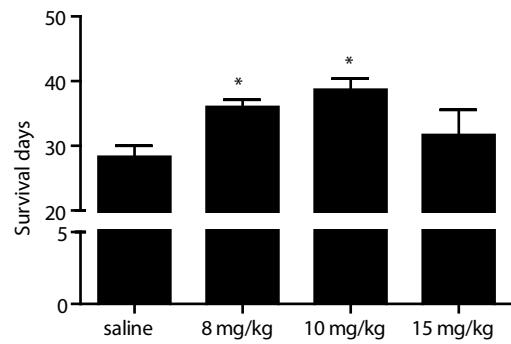
Supplementary Figure 4: Effects of albendazole on bone lesions of prostate cancer cells.
Representative (A) X-ray and (B) micro-CT images of bone lesions in the tibia of vehicle- and albendazole-treated mice. (C) Ki-67 and caspase-3 staining index from each group. Pictures show the representative H&E, Ki-67 and caspase-3 staining of bone lesions from each group.
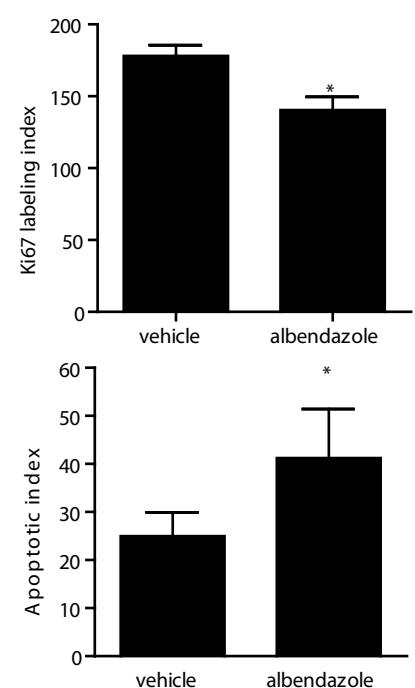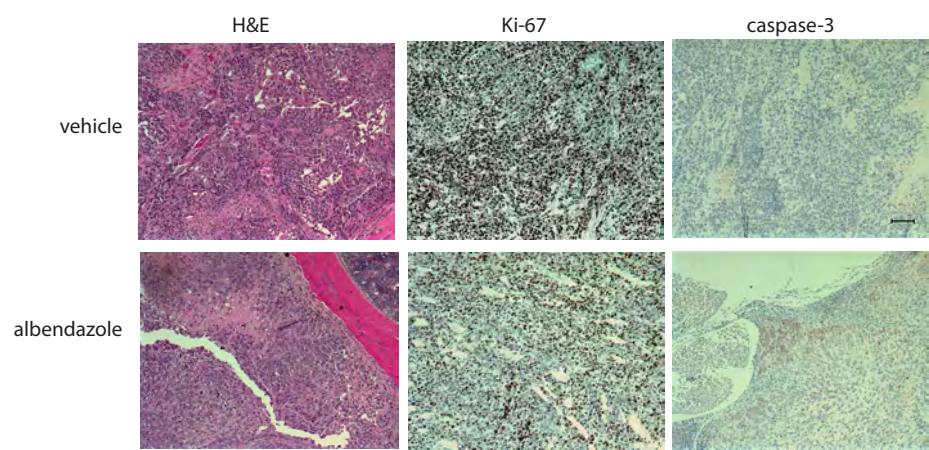
Supplementary Figure 5: Development of nanoparticle-based delivery system for albendazole

(A) Schematic of nanoparticle reagent used in this study.
(B) Optimization of nanoparticles using release kinetics study in Dunning rat AT6.1 prostate carcinoma cells.
(C) In vitro effects of albendazole formulated in nanoparticle-based vehicle in PC-3M and PC-3MLN4 cells.